3 Results

3.1 Genome-Wide Array Analysis of Normal and Malformed Human Hearts

3.1.1 Design of the Array Study

Biological and experimental variance is sometimes difficult to control in experimental studies. Therefore the experimental design is one of the most important issues in studies based on expression profiling of samples derived from different individuals. In that respect, a sufficient number of measurements must be obtained for statistical analysis of the data, either through multiple measurements of homogeneous samples (replication) or multiple sample measurements. Taking the facts given above into account, 55 cardiac samples and 6 control samples were hybridised to 61 array sets, each consisting of three array subsets, thus all together 183 array hybridisations were performed. Apart from the control samples, the gene expression profile of each sample was measured only once. The smallest statistical analysis group consisted of 4 different samples and two measurements per gene, as those were represented in duplicates on the arrays. On the biological side samples were classified according to the disease state, tissue type, gender and age. Furthermore, the hybridisations were carried out in two different hybridisation ovens. To minimise the influence of the experimental errors, each hybridisation group consisting of 4 samples was hybridised simultaneously in the same oven at one time. Two hybridisation sessions were carried out per week. Each sample received a hybridisation group number, which allowed for the statistical analysis of any of the factors mentioned above. Considering the fact that each sample was hybridised three times (one array subset per time), the different hybridisations were distributed randomly over the overall experimental time of 14 consecutive weeks to avoid a possible influence of handling variance. In addition a large control RNA batch was intermittently used as an experimental hybridisation control. An example of hybridisation groups for a three-week period is given in Table 3.1.

Disease	Tissue type	Gender	Age	Array subset	Array batch	Hyb-group
ASD	RA	M	y	1	1	1a
ASD	RA	M	o	1	1	1a
VSD	RA	M	y	1	1	1a
Normal	RA	F	o	1	1	1a
Rvdis	RV	M	y	1	1	1b
Rvdis	RV	M	y	1	1	1b
TOF	RV	M	y	1	1	1b
Normal	RV	M	o	1	1	1b
Rvdis	RV	M	y	1	2	2a
TOF	RV	M	o	1	1	2a
TOF	RV	F	y	1	1	2a
Normal	RV	M	o	1	2	2a
Normal	RA	F	o	1	1	2b
Normal	RV	M	o	1	1	2b
Normal	LV	M	o	1	1	2b
Normal	IVS	M	o	1	1	2b
ASD	RA	M	y	2	1	3a
ASD	RA	M	o	2	1	3a
VSD	RA	M	y	2	1	3a
Normal	RA	F	o	2	1	3a
ASD	RA	F	y	2	1	3b
ASD	RA	F	o	2	1	3b
TOF	RA	M	o	2	1	3b
control				2	1	3b
Rvdis	RV	M	y	2	1	4a
Rvdis	RV	M	y	2	1	4a
TOF	RV	M	y	2	1	4a
Normal	RV	M	o	2	1	4a
Normal	RA	F	o	2	1	4b
Normal	RV	M	o	2	1	4b
Normal	LV	M	o	2	1	4b
Normal	IVS	M	o	2	1	4b
ASD	RA	F	y	3	1	9a
ASD	RA	F	o	3	1	9a
TOF	RA	M	y	3	1	9a
control				3	1	9a
Normal	RA	F	o	3	1	9b
Normal	LA	F	o	3	1	9b
Normal	RV	F	o	3	1	9b
Normal	LV	M	o	3	1	9b
ASD	RA	M	y	3	1	10a
VSD	RA	M	y	3	1	10a
Rvdis	RV	M	y	3	1	10a
Rvdis	RV	F	o	3	1	10a
Rvdis	RV	F	o	3	1	10b
Rvdis	RV	F	y	3	1	10b
TOF	RV	F	o	3	2	10b
Normal	RV	F	o	3	1	10b

Table 3.1. Experimental schedule for the array study. f-female, m-male, o-old, y-young, hybridisation group-a/b assigned for the hybridisation oven used.

3.1.2 Array Optimisation and Quality Control

To check for possible production errors of each array batch, oligo hybridisations were performed for respective sub batches using $^{33}\gamma$P labelled M13 primers to visualise each M13 linked PCR product spotted on the array membrane. Thus it was possible to control each PCR product spotted on membrane. The results show that no systematic miss spotting was observed in the oligo hybridisations.

To define the optimal hybridisation conditions, various amounts of labelled total RNA (5-8µg) in combination with various exposure times (24-36 hours) were tested. 8µg directly labelled total RNA and 24 hours exposure time lead to minimal background and the highest intensities compared to 5µg total RNA and 24 hours or 36 hours exposure times.

3.1.3 Selection of Patients

To allow the selection of a balanced patient population enabling the separation of disease- or tissue-specific expression patterns, 150 samples were collected samples by a standardised procedure during cardiac surgery at the German Heart Centre Berlin. Considering known confounding factors like age and gender, 40 individuals were selected for gene expression analysis. All patients were clinically studied, and their hemodynamic state was worked up by cardiac catheterisation and echocardiography before surgery.

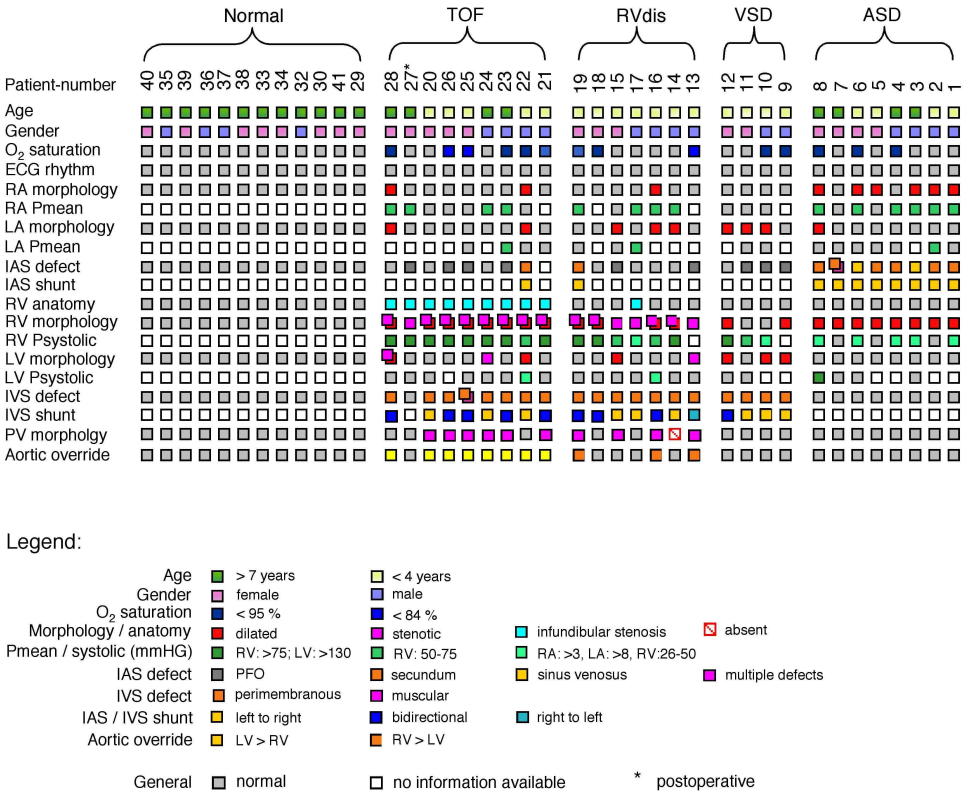

Figure 3.1. Phenotype informations of patient samples used for RNA isolation and subsequent hybridisations to array membranes.

In total, 6 normalisation samples and 55 patient samples were studied. The latter belonged to 4 categories (Figure 3.1), as follows: (1) right atrial (RA, n=2) and ventricular (n=9) samples of patients with classical Tetralogy of Fallot (TOF), exposed to pressure overload resulting in right ventricular hypertrophy; (2) right ventricular samples of a patient population (RVdis, n=7) with right ventricular hypertrophy in response to pressure overload and a variety of cardiac malformations, which were analysed together with right ventricular samples of TOF as one sample population (RVH) to elucidate the common biomechanical adaptation processes; (3) RA samples of hearts with VSD (n=4), which have not been exposed to biomechanical stress; and (4) normal RA (n=4), left atrial (LA, n=3), RV (n=6), LV (n=6), and interventricular septum (IVS, n=6) samples as well as RA samples of patients with ASD (n=8); which were profiled to identify chamber-specific genes and to provide a framework of interpretation. The normal RV, LV, and IVS samples were obtained from 6 different individuals.

Pursuing a genome-wide approach, Human Unigene Set-RZPD 2 cDNA arrays were used. The set contains 74 695 different IMAGE clones belonging to 49 255 different

Unigene clusters with 12 657 known genes representing 16 500 different Ensembl genes. In total, 9 million measurements of gene expression were made. Gene expression data is available as a supplement in the "www.molgen.mpg.de/~chd/arraywebsup/" .

3.1.4 Gene Expression Patterns and Cardiac Phenotypes

Characteristic expression patterns were obtained from a linear model analysis for the following phenotype comparisons: (A versus V) (Figure 5), the comparison of atria and ventricle, in which the analysis is based on 40 samples from different individuals (20 atria and 20 ventricles); (TOF in RV), where all 22 RV tissue samples were analysed for genes associated with TOF (9 samples); (RVH in RV), where the same 22 samples were studied for effects of right ventricular hypertrophy (16 samples); and (VSD in RA), where 18 RA samples were analysed regarding the effects of VSD (4 samples) (Table 2). The comparison between normal right and left ventricular tissue (RV versus LV), using paired *t* tests, was based on matched samples from 6 individuals. Corresponding data of each comparison can be found appendixes.

Analysed samples	**Data Set**	**TOF in RV*** (9 of 22)	**RVH in RV*** (16 of 22)	**VSD in RA*** (4 of 18)	**A vs V*** (20 vs 20)	**RV vs LV§** (6 pairs)
Clones						
	8069	323	198	215	438	149
Total (resequenced)	(3524)	(142)	(81)	(105)	(158)	(59)
Estimated false discovery rate	…….	14%	25%	23%	12%	34%
Unigene clusters	6059	264	154	178	315	117
Total (resequenced)	(3523)	(142)	(81)	(105)	(158)	(58)
Known genes	1880	86	49	86	100	53

Table 3.2. Overview of differentially expressed genes. Total numbers of cDNA clones differentially expressed in different phenotype comparisons together with the represented nonredundant numbers of Unigene clusters and known genes. The estimated false discovery rate and the number of resequenced clones are presented. The used statistical method is indicated: *Linear model; §Paired t test.

3.1.5 Verification and Comparison of Array Analysis by Real-time PCR

To verify the observed gene expression results, 21 randomly chosen genes were investigated. Relative quantification was done by the ΔΔCt method and HPRT (Hypoxanthine Phosphoribosyl Transferase) was used as a housekeeping gene for the normalisation of the expression data. $P<0.01$ was chosen for statistical confidence. As a result, 19 out of 22 genes were confirmed to be differentially expressed. The comparison

of the obtained fold-changes by array analysis versus Real-time PCR confirmed the applied array study, while in terms of fold change higher expression differences were found in the Real-time PCR analysis (Table 3.3).

		Array TOF in RV		**Real-time PCR TOF in RV**	
RZPD ID	**Gene symbol**	***P*-value**	**Fold change**	***P*-value**	**Fold change**
IMAGP956P1758	DIA	0.001128	1.6	0.014197	1.5
IMAGP956I2251	FLJ10350	0.001208	1.7	0.00073	2.7
IMAGP956A2060	LOC51189	0.006156	1.6	0.000178	4.5
IMAGP956N1316	NDUFB10	0.005818	1.5	0.026664	1.5
IMAGP956F1812	NDUFS7	0.000643	1.6	0.003288	2.3
IMAGP956I042	NHP2L1	0.005688	1.7	0.045226	1.4
IMAGP956F0258	RPL37A	0.001223	1.7	0.04457	1.7
IMAGP956K2159	S100A13	0.002023	1.6	0.015618	2.4
IMAGP956D2115	SDHA	0.000842	1.8	0.063337	1.7
IMAGP956H0722	SYTL2	0.009338	1.6	0.014637	2.2
IMAGP956G2255	TNNI1	0.000369	2.7	0.016834	24.5
IMAGP956K2055	TNNI3	0.00418	1.7	0.000176	3
IMAGP956E1912	VPS35	0.004601	1.5	0.001054	2.9
IMAGP956L2013	VWF	0.005863	1.5	0.00548	3.5
IMAGP956C23133	DPF3	0.004074	1.7	0.005970	2.5
		Array VSD in RA		**Real-time PCR VSD in RA**	
RZPD ID	**Gene symbol**	***P*-value**	**Fold change**	***P*-value**	**Fold change**
IMAGP956G1159	CALU	0.001375	0.4	0.016093	0.6
IMAGP956D0729	CFL2	0.002937	0.5	0.002371	0.4
IMAGP956D0830	COX6B	0.002685	0.5	0.119594	0.7
IMAGP956C0130	GABARAPL1	0.001851	0.2	0.001177	0.3
IMAGP956F1716	GSN	0.009865	0.4	0.071662	0.6
IMAGP956N0631	NDUFB9	0.007328	0.5	0.049669	0.6
IMAGP956A1215	PIPPIN	0.002153	0.3	0.000616	0.1

Table 3.3. Comparison of Array Analysis and Real-Time PCR of 22 randomly chosen genes.

3.1.5 Overview of Expression Levels of Different Phenotype Comparisons

To provide an overview of the molecular signatures, all known genes representing resequenced clones that appeared significantly differential ($P<0.01$) in at least one of the above comparisons [Figure 3.2, $-\log_{10}(P)$ colour-coded] were hierarchically clustered. This overview allows a comparison between the transcriptional fingerprints of each of these genes in the different phenotypes. It appears that 25% of the CHD-associated genes (green or red in one of the first 3 columns) are not chamber-specific in the normal heart (yellow in the last 2 columns).

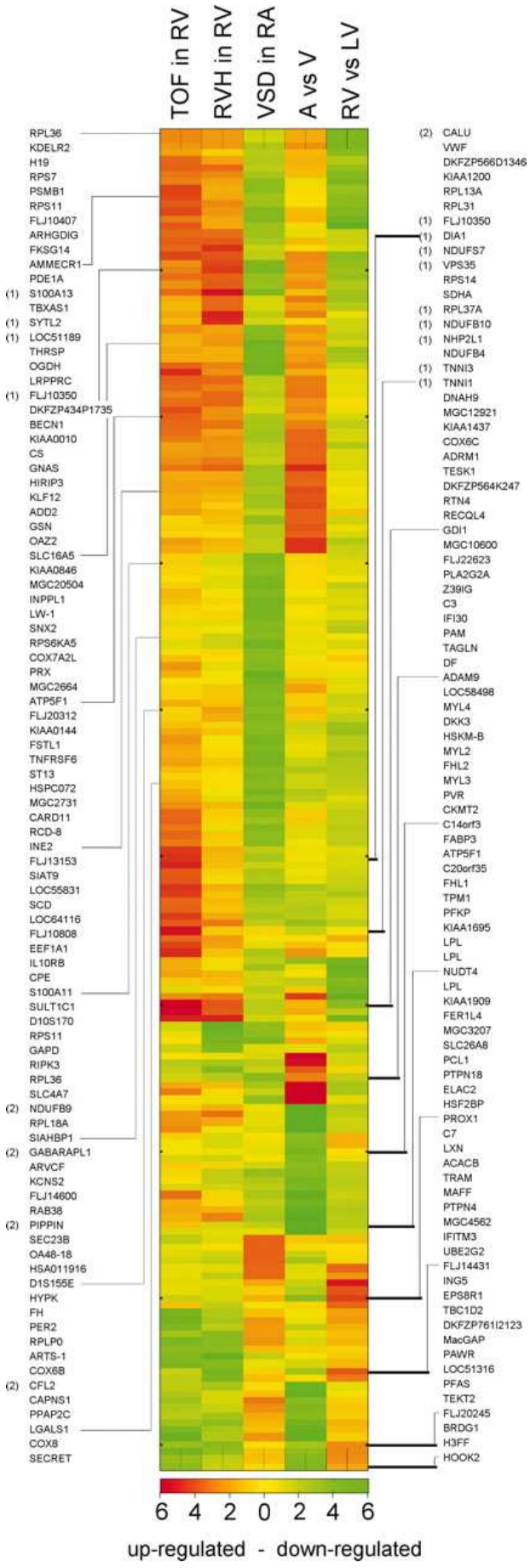

Figure 3.2. Overview of probability values and expression levels for different phenotype comparisons. Shown are all sequence-confirmed and annotated genes with $P<0.01$ in at least 1 comparison. Gene names are listed. Each comparison is represented by one column, and each gene by one row. The $-\log_{10}(P)$ of each gene in the particular comparison is colour-coded in yellow to red for upregulated and yellow to green for downregulated genes. For example, a value of 2 stands for $P=0.01$ and is colour-coded in red if the gene is upregulated. The differentially expressed genes confirmed by Real-time PCR are indicated with 1 if tested for TOF in RV and 2 if tested for VSD in RA

Additional inspection reveals a partially similar expression dynamic of the TOF portrait with that of RVH but an opposite expression dynamic compared with VSD.
In addition, large amounts of genes characteristic for the molecular signature of VSD are not differentially expressed in any other analysis. Comparison of the expression profile of genes characteristic for TOF and RVH provides the possibility of subtracting both from each other and identifies genes specific for either TOF or RVH.

3.1.6 Association of Functional Gene Categories to Specific Phenotypes

To provide a global view of the association of functional gene categories with particular phenotypes, correspondence analysis (Fellenberg et al. 2001) was used as a statistical method (Figure 3.3). Clones were assigned to gene ontology categories according to the annotations in the LocusLink database. Correspondence analysis was applied to the contingency table of numbers of differentially expressed genes ($P<0.05$) per gene ontology category and phenotype comparison. Gene categories with similar patterns of regulation across phenotypes are mapped close to each other. Furthermore, the biplot shows the associations between gene categories and phenotypes. A gene category lies far in the direction of a certain phenotype, if disproportionally many genes are differentially expressed in this phenotype. For instance, many genes contributing to the structural integrity of a muscle fibre (structural constituent of muscle) are differentially expressed between atria and ventricle.

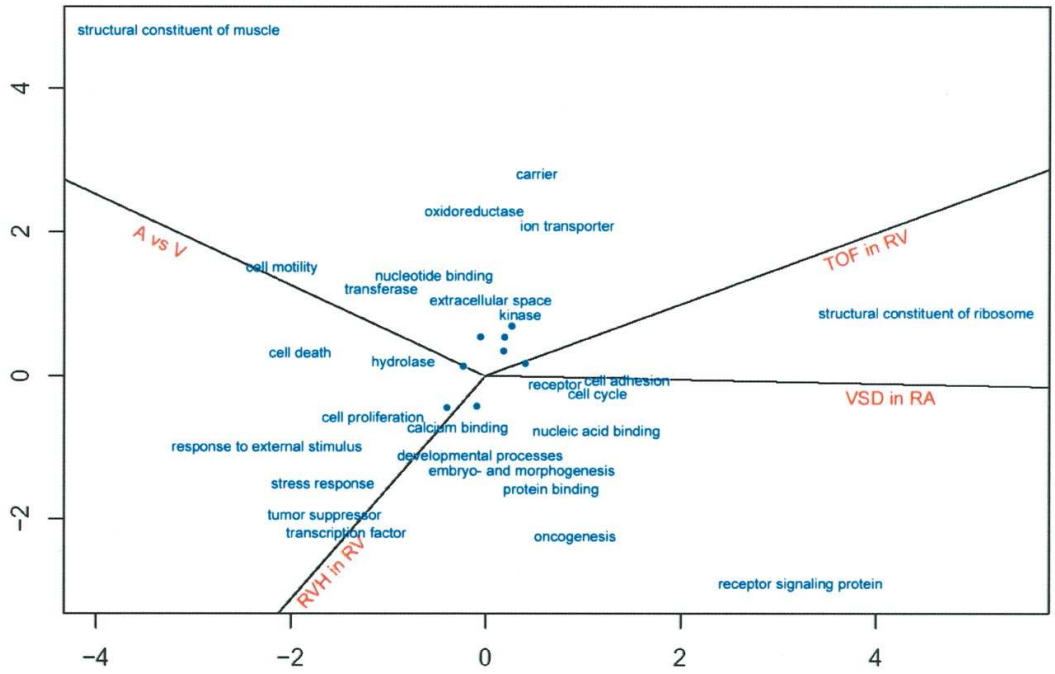

Figure 3.3. Biplot obtained from correspondence analysis. The plot shows the association between gene ontology categories (blue) and phenotypes (red) with respect to differential gene expression. The gene ontology categories belong to the 4th level of granularity, allowing a detailed but not diverse functional description. Categories that are not specifically associated with any phenotype are represented by dots.

3.1.7 Class Discovery Using ISIS

The class discovery method called ISIS was used in order to see which class distinctions among the tissue samples are most pronounced in terms of gene expression profiles. The most outstanding binary class distinction identified by ISIS, irrespective of sample annotations, was exactly the distinction between atrium and ventricle samples.

3.1.8 Atrium versus Ventricle

Since the human heart consists of two general compartments, the atria and ventricles, each of them was analysed separately and their expression patterns compared to obtain the distinct molecular portraits of both atria and ventricles. In total, 438 clones were found to be differentially expressed (P<0.01) corresponding to 315 Unigene clusters and 100 known genes. In addition to well-known chamber-specific genes, like atrial and ventricular myosin light chains, this signature includes diverse, previously unknown chamber-specific genes for muscle contraction, extracellular components, and cell growth and differentiation and energy metabolism.

The less force-developing atria were characterised by higher expression of genes encoding proteins associated with extracellular matrix or actin modulation, like CST3

and PCOLCE. The translation factors EEF1A and the DNA helicase REQL4 were highly significantly upregulated in the atria. Also, KCNIP2 is highly overexpressed in the human atria compared to the ventricles (P=0.01).

Genes with higher expression levels in ventricles compared to atria belong mainly to 3 major functional classes: cytoskeleton-contraction, metabolism–energy turnover, and cell cycle–growth. Several of these genes are involved in ventricular myocardial disorders such as TMP1, ANKRD2 and FHL1, which has been shown to be downregulated in failing human hearts (Yang et al. 2000; Karibe et al. 2001; Pallavicini et al. 2001).

The combination of computational analysis of protein similarity together with genome-wide transcription footprint of the heart points to so far functionally unknown genes. For instance, Unigene cluster Hs.355815, which has a 59% protein sequence similarity to the myotonic dystrophy-associated protein kinase ß in rat, specifically expressed in ventricle.

3.1.9 Left Ventricle versus Right Ventricle

In addition to atrial and ventricular specifications, normal high-pressure and low-pressure were analysed for molecular differences (Table 3.2, Figure 3.2), a complete list of genes from this comparison is shown as a table in the appendix and 149 clones were found to be differentially expressed corresponding to 117 Unigene clusters and 53 known genes. As a result of the analysis, genes encoding proteins involved in cell cycle, cell differentiation, and energy metabolism were found to be downregulated in the RV compared to the LV. An example of new information derived from the analysis is the LV-specific expression of Unigene cluster Hs.323099 sharing a sequence similarity of 93% to ALK3, which is essential for cardiac development (Gaussin et al. 2002). Furthermore, there was no significant difference observed between LV and IVS.

3.1.10 Tetralogy of Fallot and Right Ventricular Hypertrophy

TOF and RVH showed distinct molecular portraits with genes of various functional classes. Even though the right ventricular hypertrophy is part of TOF, two gene expression profiles could clearly be distinguished when comparing only TOF samples and TOF samples combined with the RVdis samples as one phenotype (RVH). Therefore, TOF reveals the molecular signature of the malformation in addition to the adaptation portrait. For the TOF comparison, 323 clones were found to be differentially

expressed corresponding to 86 known gene. In contrast to TOF, RVH showed only 198 differentially expressed clones corresponding to 49 known genes.

In addition to genes involved in cell cycle, a characteristic feature of the TOF signature is the upregulation of the ribosomal proteins S6, L37a, S3A, S14, and L13A (Figure 3.5A). Results of expression data reveal a TOF-specific dysregulation of potential targets that could be involved in pathways leading to cardiac dysdevelopment (Figure 3.5A) as for example SNIP, A2BP1, KIAA1437 and CERD4. In addition, genes markedly downregulated in TOF include STK33, BRDG1 and TEKT2.

RVH showed a hypertrophy-specific gene expression pattern of genes mainly involved in stress response, cell proliferation, and metabolism. Interestingly, we detected the upregulation of ADD2, whose relative ADD1 was recently shown to be associated with hypertension in human (Nishimura et al. 2002).

Since the expression of several genes of the RVH signature was similar to their expression levels in the LV (Figure 3.2), the next analysis focused on whether the molecular adaptation to pressure overload could lead to a molecular transition from right to left ventricular characteristics. For the RVH-associated genes ($P<0.01$), the difference between the mean intensity of each gene in RVH and that in normal RV samples to the mean intensity of the gene in normal LV samples was compared and a significantly positive correlation coefficient of 0.27 ($P<0.0001$, permutation test) was found, indicating that the genes dysregulated in RVH have a tendency to behave similar in the disease state as in normal LV tissue (Figure 3.4).

To separate the malformation from the adaptation-specific molecular signature in TOF, RVH-specific genes were subtracted from the TOF molecular portrait. All genes with $P<0.1$ in RVH were subtracted from all genes with $P<0.01$ in TOF, resulting in 88 clones corresponding to 35 known genes highly specific for TOF with regard to the primary changes underlying the malformation process (see appendix for gene lists).

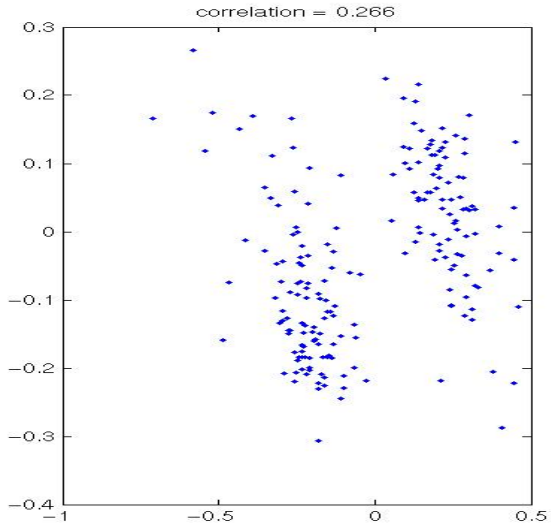

Figure 3.4. Genes dysregulated in RVH behave similarly in normal LV tissue (Genes associated with RVH (P<0.01)). X-axis: difference between mean expression levels in RVH and those in RV samples; Y-axis: mean expression levels in normal LV samples.

3.1.11 Ventricular Septal Defect

To obtain a molecular portrait that is not influenced by biomechanical adaptation processes, RA samples of patients with VSD, intact tricuspid valve, and normal RA pressure were studied. 215 clones corresponding to 86 known genes were found to be differentially expressed. It was observed that the VSD-specific molecular signature is dominated by downregulated genes compared to the other RA samples (Figure 3.5B). As seen in TOF, several ribosomal proteins such as S11, L18A, L36, LP0, L31, and MRPS7 are differentially expressed, but here they are downregulated. It was observed that, expression of ion channel genes was restricted to solute and potassium channels; for instance, SLC26A8, SLC16A5, SLC4A7, KCNS2, and KCNN3. A thorough literature study of downregulated genes in VSD revealed that a major part is involved in cell proliferation and differentiation during embryogenesis as well as apoptosis. Examples are AMD1, RIPK3, EGLN1, SIAHBP1 and ARVCF that are found to be significantly downregulated.

3.1.12 Genome Wide Compendium of Persistent Human Heart Transcripts

In addition, a set of 6075 clones (4340 different Unigene clusters) appeared to be persistently transcribed in the analysed samples. Data can be reached from the following web address “http://www.molgen.mpg.de/~chd/arraywebsup”.

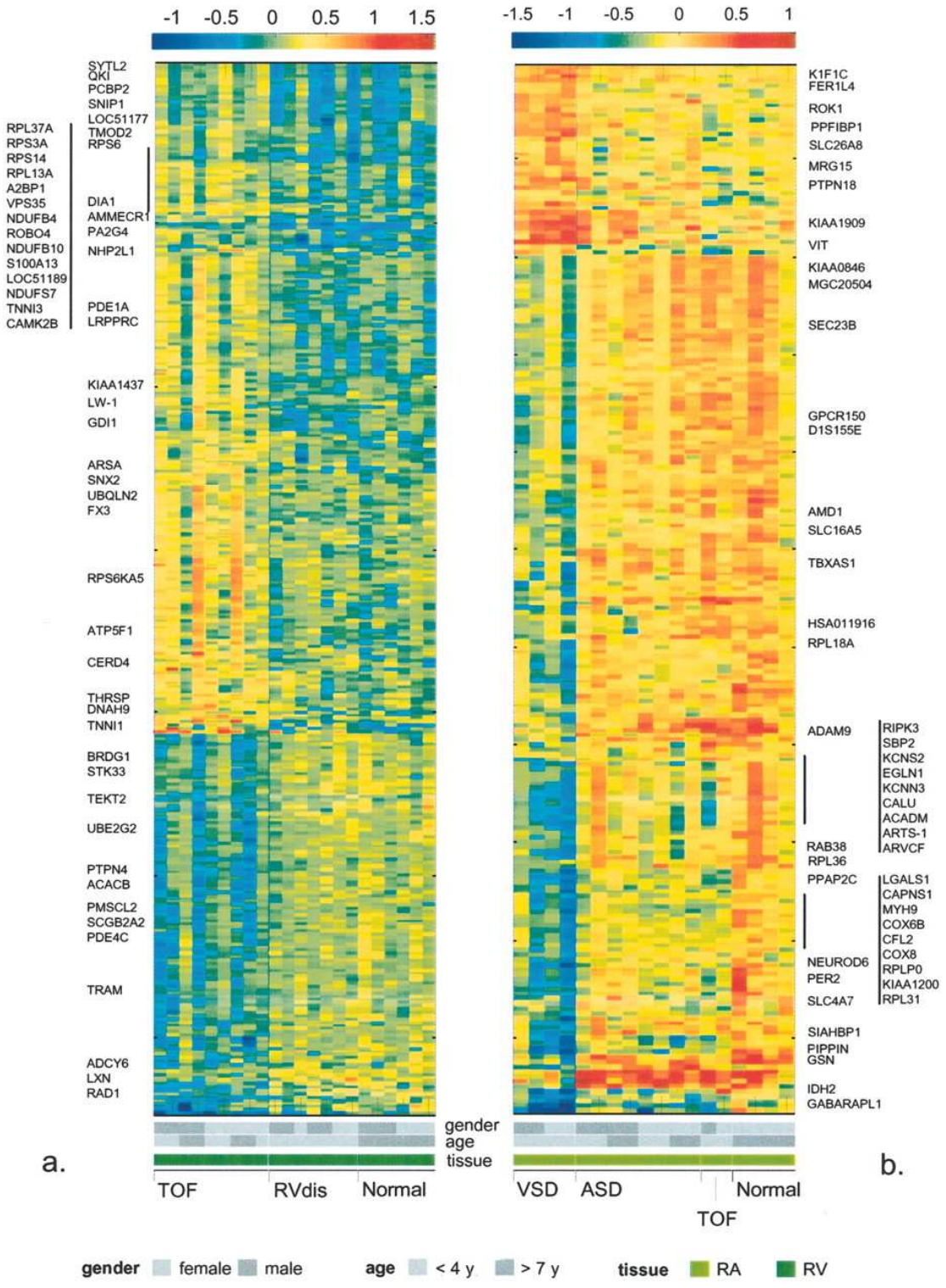

Figure 3.5. Hierarchical clustering of differentially expressed genes in TOF in RV (a) and VSD in RA (b). Shown are the expression patterns of genes associated with TOF and VSD compared with the other samples from the same cardiac chamber. Each column represents a single patient and each row a single clone. Normalised expression levels of clones with $P<0.01$ are colour-coded for each sample. For examples of annotated genes, gene symbols are listed. The phenotype information for gender, age, tissue, and disease state is indicated.

3.2 Spatio-temporal Characterisation of Selected Genes

3.2.1 Whole Mount *in situ* Hybridisation Screen on Mouse Embryos

Following the Real-Time confirmation of randomly selected genes, a whole mount *in situ* hybridisation analysis of selected genes was performed to prove the functional relevance of differentially regulated genes during early cardiac development. The selection was based upon genes with potential DNA binding domains or highly expressed genes that were not characterised previously in early development in terms of its expression pattern.

Considering the two particular criteria above, TNNI3 (troponin I) causative for hypertrophic cardiomyopathy (HCM); CFL2 (cofilin) with actin-binding domains; Calu (Calumenin) with EF-hand binding domains and DPF3 (Cerd4) with double PHD and C2H2 type zinc finger domains were selected for whole mount *in situ* hybridisations.

TNNI3

TNNI3, known as cardiac troponin I, is localised on chromosome 19q13.4 in human**.** TNNI3 mutations are the cause of familial hypertrophic cardiomyopathy 7 (MIM: 191044). Hypertrophic cardiomyopathy is a cardiac disorder characterised by ventricular hypertrophy that is frequently asymmetric and often involves the interventricular septum. The prevalence of the disease in the general population is 0.2%. TNNI3 represents the inhibitory subunit of troponin, the thin filament regulatory complex that confers calcium-sensitivity to striated muscle actomyosin-ATPase activity. Mouse Tnni3 is located on chromosome 7 (GI: 484093). A 399bp fragment corresponding to base 115 through 513 of accession number U09181 was synthesised as RNA *in situ* hybridisation probe from adult mouse heart cDNA. Tnni3 was hybridised to E8.5, E9.5 and E11.5 embryos. At E8.5 embryos, expression is restricted to the heart tube, inflow and outflow tract; at E9.5, the expression of Tnni3 remained at the common atrium as well as ventricle and the atrioventricular channel. At E12.5, where four chambers can clearly be distinguished, expression of Tnni3 was observed in all chambers (Figure 3.6A-C).

CFL2

Human CFL2 (cofilin muscle) has been mapped to chromosome 14q13.1 and has two splice forms, CFL2a and CFL2b, derived from differential splicing of the first exon. On the protein level CFL2 has an actin-binding domain (Interpro: IPR002108, cofilin/tropomyosin type) and belongs to the AC protein family. AC proteins are involved in cytokinesis, cell movement, endocytosis and all processes associated with actin dynamics. In vitro, cofilin has a pH-dependent actin depolymerisation activity. At pH< 7.0, cofilin binds in a 1:1 ratio to F-actin and cosediments with actin filaments. At pH>7.0, AC proteins increasingly depolymerise F-actin yielding a 1:1 complex of monomeric actin and AC protein (Mohri et al. 2000; Thirion et al. 2001). For the Mouse ortholog Cfl2 [GI: 139398043] on chromosome 12, a 328bp RNA *in situ* hybridisation probe was synthesised corresponding to the BC007138 sequence (1001-1328bp) and hybridised to E8.5, E9.5 and E10.5 mouse embryos. Cfl2 expression was observed in allantois, frontal nasal process, hindbrain and throughout the ectoderm of the lateral and posterior body at E8.5. At E9.5 expression was observed in somites, telencephalon and the first branchial arch, whereas at E10.5 a weak Cfl2 expression could be observed at atrial and ventricular components of the heart and limbs (Figure 3.6 D-F).

CALU

Human CALU (Calumenin) is linked to chromosome 7q32.1 and has two splice forms with 92% amino acid identity obtained through differential splicing of two alternative second exons. It is one of the members of Ca^{2+} binding CREC family, which has been identified to contain multiple EF-hands and a C-terminal endoplasmic reticulum retention signal leading to their physical localisation to the endo/sarcoplasmic reticulum of mammalian hearts. The rhythmical contraction of cardiac myocytes is maintained by the strict regulation of their cytoplasmic Ca^{2+} concentration. To achieve this regulation, cardiac myocytes develop their specialised ER, called the sarcoplasmic reticulum, as the Ca^{2+} storage compartment with rhythmical Ca^{2+} oscillation between the sarcoplasmic reticulum and the cytosol. Previous studies showed that Calumenin is most strongly expressed in the adult heart and E18.5 whole embryos in RT-PCR experiments (Jung et al. 2004). The mouse ortholog Calu [GI: 31982481] is located on chromosome 6. Its genomic organisation is similar to human CALU and the two alternative second exons determine the isoform. A 374bp RNA *in situ* hybridisation probe was prepared from a mouse adult heart cDNA corresponding to the NM_007594 sequence (2648-3021bp)

and hybridised to E8.5 and E10.5 mouse embryos. At E8.5, Calu is ubiquitously expressed throughout the embryonic body. In contrast, at E10.5, ventricles as well as atria, forelimbs, first and second branchial arches were stained (Figure 3.6G-H).

DPF3

DPF3 (Cerd4) is localised on 14q24.3-q31.1 in human, and characterised by a double PHD domain and a C2H2 type zinc finger domain indicating its potential function as a DNA-binding transcription factor. DPF3 belongs to the D4 gene family. Previous studies suggested that DPF3 is involved in the development of the nervous system (Ninkina et al. 2001). A 346bp RNA *in situ* hybridisation probe corresponding to the NM_058212 sequence (833-1178bp) was hybridised to E8.5 and E10.5 embryos. Expression was observed at E8.5 in the ventricle, the inflow tract covering the sinoatrial region of the early heart and the presomitic mesoderm. E10.5 embryos showed expression in telencephalon, midbrain, rhombencephalon, somites, left and right atrium, outflow tract and in the eyes.

With regard to this expression profile during early cardiac development, Dpf3 was selected for a detailed functional characterisation described in the following chapters.

Figure 3.6. WHISH expression analysis of 4 selected genes. Figure 9A-C mouse embryonic stages E8.5, E9.5, E12.5 were hybridised with Tnni3 RNA-ISH probe: E8.5 ventral view, E9.5 left view, E12.5 left view. nf-neural fold, ht-heart tube, ift-inflow tract, v-ventricle, a-atrium, rv-right ventricle, lv-left ventricle, la-left atrium. D-F mouse embryonic stages E8.5, E9.5, E11.5 were hybridised with Cfl2 RNA-ISH probe: E8.5 ventro-lateral view, E9.5 left view, E11.5 left view. mb-mid brain, hb-hind brain, fnp- frontal nasal process, al-allantois, som-somite, tlc-telencephalon, fba-first branchial arch, la-left atrium fl-forelimb. G-H mouse embryonic stages E8.5 and E11.5 were hybridised with Calu RNA-ISH probe: E8.5 ventro-lateral view, E11.5 left view. fnp-frontal nasal process, lv-left ventricle, la-left atrium, fl-forelimb, fba-first branchial arch, sba-second branchial arch. J-K mouse embryonic stages E8.5 and E10.5 were hybridised with Cerd4 (Dpf3) RNA *in situ* probe: E8.5 ventro-lateral view, E10.5 left view. v-ventricle, ift-inflow tract, mb-mid brain, tlc-telencephalon, e-eye, rhm-rhombomer (rhombencephalon), som-somite, oft-outflow tract, lv-left ventricle, la-left ventricle. I, L mouse embryonic stages E9.5 and E10.5 were hybridised with Nkx-2.5 (used as a heart marker), v-ventricle, oft-outflow tract, avc-atrioventricular channel, a-atrium, rv-right ventricle, lv-left ventricle, la-left atrium.

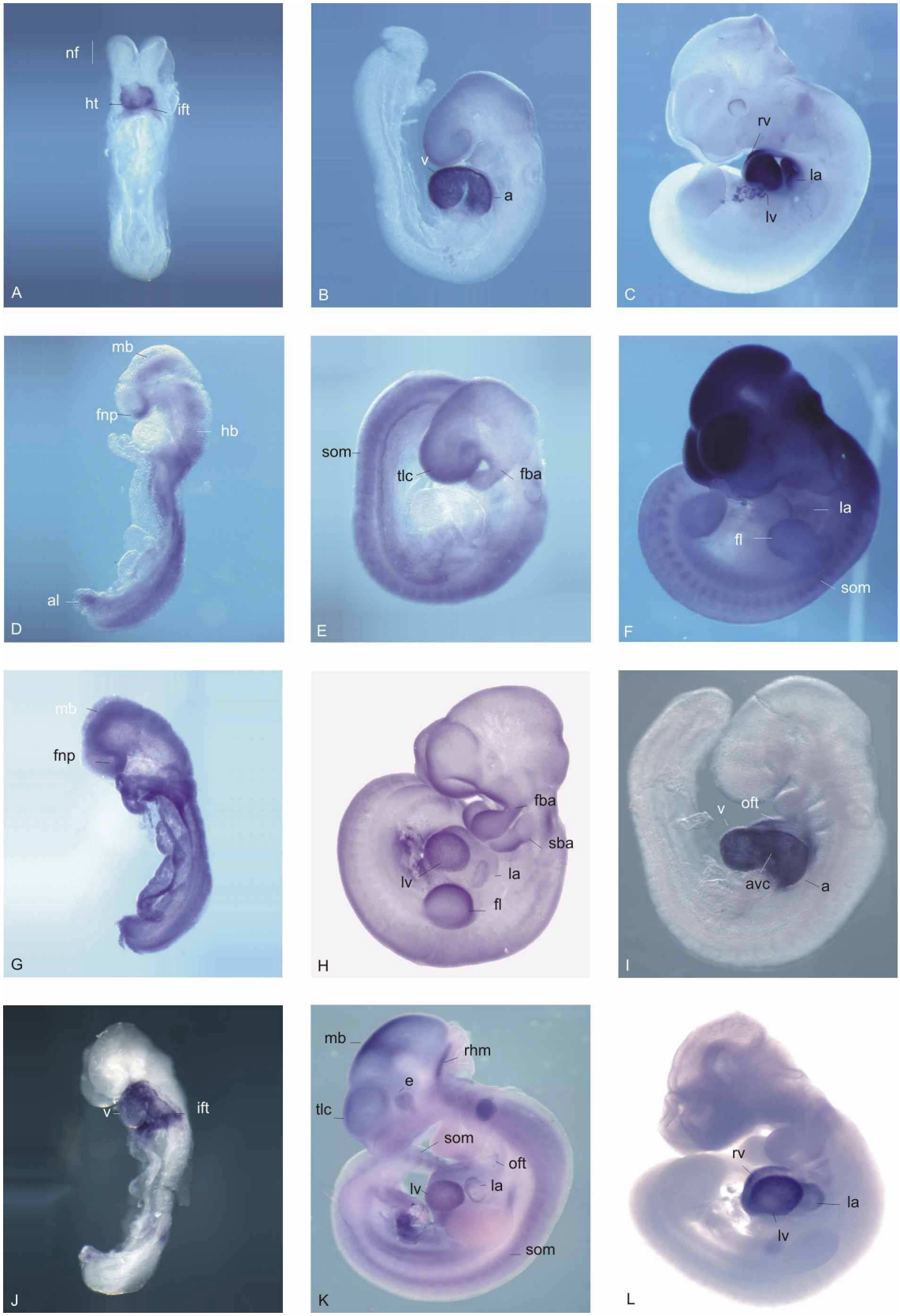
nf
ht
ift
A
v
a
B
rv
la
lv
C
mb
fnp
hb
al
D
som
tlc
fba
E
la
fl
som
F
mb
fnp
G
fba
sba
lv
la
fl
H
v
oft
avc
a
I
v
ift
J
mb
rhm
e
tlc
som
oft
lv
la
som
K
rv
la
lv
L

Figure 3.6

3.2.2 Human DPF3 Splice Variants

Human DPF3 (CERD4) is the third member of the D4 gene family. Genes of the D4 family (Ninkina et al. 2001), DPF1, DPF2 and DPF3 have previously been described as specifically expressed in brain and nervous system and share DNA binding domains; a C2H2 type zinc finger domain and a double PHD finger domain. In general all D4 family members are highly similar at the protein level as pointed out in figure 10. DPF3 is localised on chromosome 14 and has two known splice variants according to GeneBank BC026305 (DPF3/1) and NM_012974 (AK02414, DPF3/3) consisting of 6 and 10 exons, respectively. A further human splice variant, consisting of 11 exons and corresponding to mouse splice variant AK039011 (DPF3/2), was cloned by Grimm *et al* (AY803021) (Figure 3.11).

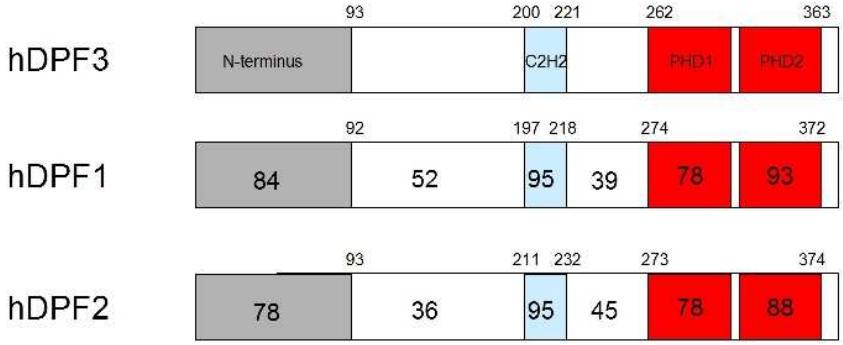

Figure 3.7. D4 family multiple alignment of protein sequences. Numbers correspond to % of identical amino acids.

To initially characterise the human DPF3 gene, PCRs were performed on human adult heart cDNA and human genomic DNA. The full-length transcript of DPF3/3 corresponding to NM_012974 could not be amplified whereas DPF3/1 and DPF3/2 were obtained as full-transcripts (data not shown).

Furthermore a series of Northern Blot hybridisations were performed using the human Clontech NTM™ 12 lane multiple tissue blot. Using a ^{32}P labelled 358bp cDNA probes representing the common region of the DPF3 gene, two specific splice variants were identified at the heart and skeletal muscle lanes (Figure 3.8). A ^{32}P labelled β-actin cDNA was hybridised as a control probe onto the same membrane after stripping. Here, a 2kb signal in all tissues and a 1.8kb signal at the heart and skeletal muscle lanes were identified as stated by Clontech (PT1200-1; PR12172 User manual).

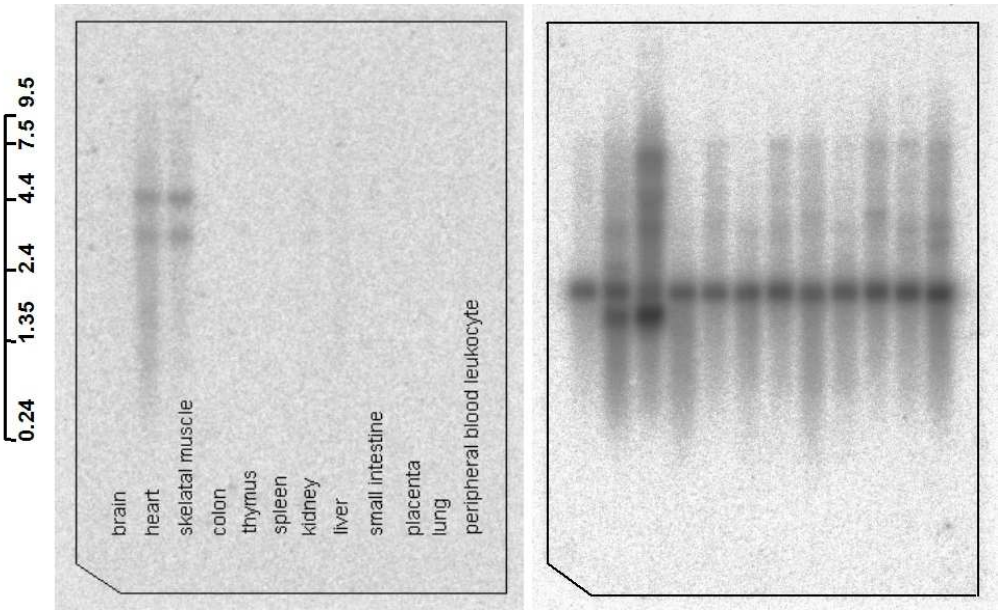

Figure 3.8. Human 12 tissue Northern Blot was hybridised with ^{32}P labelled DPF3 common region probe (on the left). The same membrane was hybridised with ^{32}P β-actin cDNA following the stripping (on the right).

3.2.3 Quantification of Human DPF3 Gene Splice Variants in Normal and Malformed Hearts

The expression level of the human DPF3 splice variants were analysed in detail by Real-time PCR in right ventricular samples of TOF patients and normal healthy hearts and quantified by the ΔCt method. In addition, the expression levels of the two human splice variants were compared to each other in normal hearts (Figure 3.9).

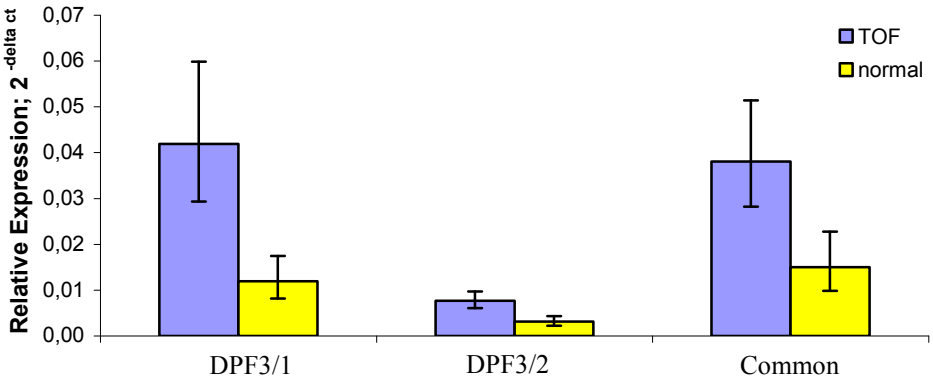

Figure 3.9. Expression of DPF3 splice variants in human heart: Real-time PCR analysis was performed on RV samples of TOF patients and normal healthy hearts. Primers specific for the DPF3/1-splice variant, the DPF3/2-splice variant and the common-shared region of DPF3 were used as indicated and the results normalised to expression of beta-2-microglobulin using the ΔCt method.

B2M (beta-2-microglobulin) was used in relative quantification as a housekeeping gene. Both splice variants of DPF3 were upregulated in TOF malformed hearts compared to normal hearts. Further a comparison between the two different transcripts revealed a 3.8 fold higher upregulation of splice variant 1 (DPF3/1) compared to splice variant 2 (DPF3/2) in TOF derived hearts. In normal adult hearts the expression level of DPF3/1 was 2.5 fold higher than the expression level of DPF3/2.

3.2.4 Mouse Dpf3 Splice Variants

Mouse Dpf3 is distributed over a region of approximately 75Mb on chromosome 12 (Ensembl v29) and has two characterised transcripts: NM_058212 contains 9 exons, and corresponds to the human splice variant DPF3/1 and will therefore in the following be called Dpf3/1. AK039011 contains 11 exons, corresponding to the human splice variant DPF3/2 and will be called Dpf3/2. The first 8 exons of both transcripts are highly conserved (Figure 3.11). Whereas Dpf3/1 is terminating with exon 9, Dpf3/2 harbours exon 11 through exon 13, comparable to the human homologue. As in human, mouse Dpf3 has a C2H2 type zinc finger domain spanning exon 6 through exon 7, that is therefore contained in both splice variants. Moreover, in Dpf3/2 a PHD finger domain. Is spanning from exon 8 to exon 11 and a second PHD finger domain covers exon 11 through 13. Due to the lack of exons 9, 11, 12 and 13 the splice variant Dpf3/1 only contains half of a PHD finger. These features of Dpf3 are conserved in other species including human and chicken (Figure 3.11).

At protein level, multiple alignments of mouse D4 proteins show conserved C2H2 type zinc finger domains and a very similar double PHD finger domain, although DPF1 is lacking three amino acids in the beginning of the first PHD finger domain. Comparisons of similarity scores of amino acid sequences reveal that human and mouse D4 family members are highly homologous and conserved in evolution (Table 3.4, Figure 3.10).

```
Mouse DPF1 MATVIPSPLS-LGEDFYREAIEHCRSYNARLCAERSLRLPFLDSQTGVAQNNCYIWMEKT 59
Mouse DPF3 MATVIHNPLKALGDQFYKEAIEHCRSYNSRLCAERSVRLPFLDSQTGVAQNNCYIWMEKR 60
Mouse DPF2 MAAVVENVVKLLGEQYYKDAMEQCHNYNARLCAERSVRLPFLDSQTGVAQSNCYIWMEKR 60

Mouse Dpf1 HRGPGLAPGQIYTYPARCWRKKRRLNILEDPRLRPCEYKIDCEAPLKKEGGLP-EGPVLE 118
Mouse Dpf3 HRGPGLAPGQLYTYPARCWRKKRRLHPPEDPKLRLLEIKPEVELPLKKDGFTS-ESTTLE 119
Mouse Dpf2 HRGPGLASGQLYSYPARRWRKKRRAHPPEDPRLSFPSIKPDTDQTLKKEGLISQDGSSLE 120

Mouse Dpf1 ALLCAETGEKK--VELKEEE------TIMDCQKQQLLEFPHDL----EVEDLEEDIPRRK 166
Mouse Dpf3 ALLRGEGVEKK--VDAREEE------SIQEIQR--VLENDENVEEGNEEEDLEEDVPKRK 169
Mouse Dpf2 ALLRTDPLEKRGAPDPRVDDDSLGEFPVSNSRARKRIIEPDDFLDDLDDEDYEEDTPKRR 180

Mouse Dpf1 NRARGKAYGIGGLRKRQDTASLEDRDKPYVCDICGKRYKNRPGLSYHYTHTHLAEEEGEE 226
Mouse Dpf3 NRTRGRARGSAGGRRRHDAASQEDHDKPYVCDICGKRYKNRPGLSYHYAHTHLASEEGDE 229
Mouse Dpf2 GKGKSKSKGVSSARKKLDASILEDRDKPYACDICGKRYKNRPGLSYHYAHSHLAEEEGED 240

Mouse Dpf1 HTER--HALPFHRKNNHKQFYKELAWVPEAQRKHTAKKAPDGTVIPNGYCDFCLGGS--- 281
Mouse Dpf3 AQDQETRSPPNHRNENHR-----------------PQKGPDGTVIPNNYCDFCLGGSNMN 272
Mouse Dpf2 KEDSRPPTPVSQRSEEQK-----------------SKKGPDGLALPNNYCDFCLGDSKIN 283

Mouse Dpf1 KKTGCPEDLISCADCGRSGHPSCLQFTVNMTAAVRTYRWQCIECKSCSLCGTSENDDQLL 341
Mouse_Dpf3 KKSGRPEELVSCADCGRSGHPTCLQFTLNMTEAVKTYKWQCIECKSCILCGTSENDDQLL 332
Mouse Dpf2 KKTGQPEELVSCSDCGRSGHPSCLQFTPVMMAAVKTYRWQCIECKCCNLCGTSENDDQLL 343

Mouse Dpf1 FCDDCDRGYHMYCLSPPMAEPPEGSWSCHLCLRHLKEKASAYITLT-- 387
Mouse Dpf3 FCDDCDRGYHMYCLNPPVAEPPEGSWSCHLCWELLKEKASAFGCQA-- 378
Mouse Dpf2 FCDDCDRGYHMYCLTPSMSEPPEGSWSCHLCLDLLKEKASIYQNQNSS 391
```

Figure 3.10. Alignment of the amino acid sequences of the mouse D4 family: Dark grey shaded blocks represent the N-terminal site, blue letters in grey shade correspond to the C2H2 type zinc finger domain and red letters in light grey shade highlight the PHD finger domains.

	hDPF1	**hDPF2**	**hDPF3**
mDPF1	**84/85**		
mDPF2		**98/99**	
mDPF3			**99/99**

Table 3.4. Comparison of amino acid identity/similarity of mouse versus human DPF genes: The numbers represent % amino acid identity / % amino acid similarity.

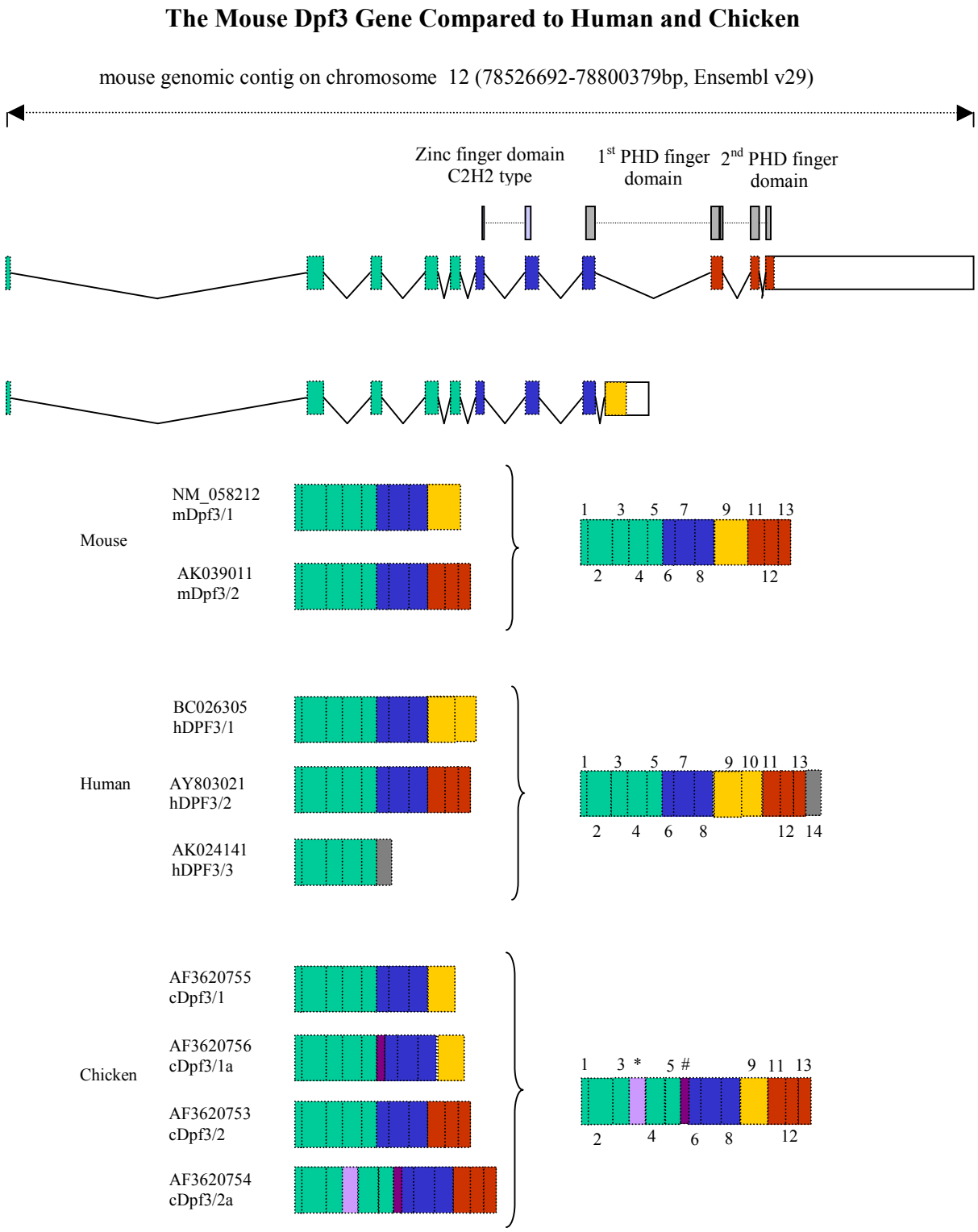

Figure 3.11. Comparison of DPF3 splice variants in human and chicken in comparison to the mouse genomic locus. Boxes represent individual exons independent from their colours (for chicken *, # signs indicate extra sequences). On the left, splice variants with similar exon sequence were grouped together, on the right side, the genomic order of all appearing exons is grouped together for each species. The top part shows the genomic organisation of the mouse (exons and introns were scaled independently to represent a global overview).

3.2.5 Quantification of Dpf3 Splice Variants in Early Developing Mouse Heart

The expression levels of the two known mouse splice variants of Dpf3 were quantified with semi-quantitative RT-PCR using E9.5 day heart cDNA. As seen in figure 15 and obtained through densitometry, Dpf3/1 shows a more than 2 fold higher expression in embryonic mouse hearts than Dpf3/2 (Figure 3.12).

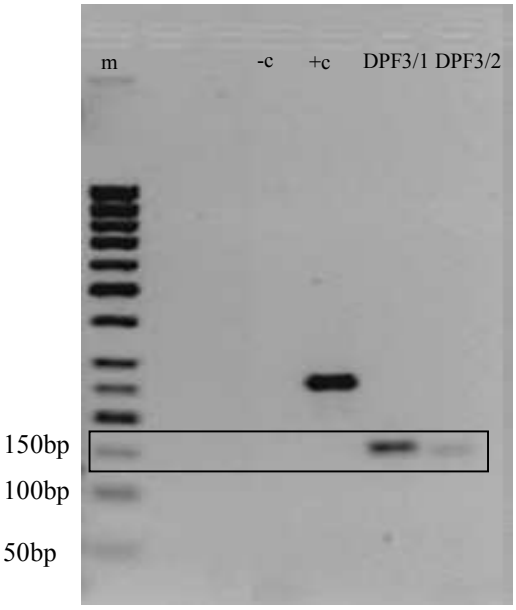

	Marker	Dpf3/1	Dpf3/2
ln(densitometry)	1.44	2.52	1.13
Normalised	1	1.75	0.78
Ratio (Dpf3/1/Dpf3/2)		2.24 fold	

Figure 3.12. Left panel gel: RT-PCR of mouse Dpf3 splice variant 1 and 2 from E9.5 mouse heart RNA. m-marker lane, -c – negative control, +c – positive control, Dpf3/1, Dpf3/2 . Right panel: normalisation of densitometry.

3.2.6 Expression Pattern of Dpf3 During Mouse Development

To analyse the expression pattern of Dpf3 in mouse embryonic stage E7.5, E8.0, E9.5, E10.5 embryos and extracted hearts (E10.5 and E12.5) were used for whole mount *in situ* hybridisation. Three different DIG-labelled RNA *in situ* hybridisation probes were generated covering the common region (common), and the Dpf3/1 and Dpf3/2 specific regions, respectively. The aim was to distinguish the expression patterns of the different splice variants.

At E7.5 restricted expression was observed at the cardiac crescent, where the heart is initiated from the lateral mesoderm bands, for the common (Figure 3.13A) and Dpf3/1 specific probes (Figure 3.13D). Furthermore, the allantois was stained with both probes. Dpf3/2 (Figure 3.13G) was not expressed at this stage. At E8.0, heart tube, outflow tract, inflow tract and presomitic mesoderm were stained for the Dpf3/1 (Figure 3.13E,

F, G) and the common probes (Figure 3.13B, C). Again, Dpf3/2 was not expressed at this stage. At E8.5, Dpf3/1 (Figure 3.13J) and common (Figure 3.13K) region specific probes showed expression in the cardiac region including inflow tract, heart tube, outflow tract, atrium, ventricle, septum transversum, presomitic mesoderm, youngest somites and allantois. Dpf3/2 (Figure 3.13L) did not show any specific expression. At E9.5, the heart shows more distinct morphology compared to previous stages; a common atrium and ventricle are distinguishable. Similar expression patterns have been seen for the common (Figure 3.14A,B) and the Dpf3/1 (Figure 3.14D,E) probes; common atrium and ventricle, atrioventricular channel, sinus venosus (including inflow tract), septum transversum and youngest somites were stained. In addition, the future midbrain showed staining with the common probe at this stage. Using the Dpf3/2 probe, only the septum transversum was stained. Further, E9.5 embryos that were already hybridised with the common probe, were embedded in gelatine and sagitally sectioned (50μ thick) with vibratome equipment for further inspection. The section in figure 17K shows the left side of the embryo. Expression was observed in the common ventricle, the left sinus horn (belonging to the sinus venosus), the common atrium, the atrioventricular channel, the outflow tract, the septum transversum, the intraembryonic coleom cavity and its linings including the gut. In Section-II passing on the right side of the embryo (Figure 3.14J), the same observations remained. In addition a mild expression was observed through the optic vesicle. The expression of Dpf3 at E10.5 became weaker in the heart compared to previous stages. The common (Figure 3.14C) and the Dpf3/1 (Figure 3.14F, L) specific probes gave staining at the lateral walls of the ventricles, the atria, and the atrioventricular channel and very weakly at the outflow tract, the first somites and in the mid brain. For the Dpf3/2 probe (Figure 3.14I) staining was observed in midbrain (a shared feature with the common and the Dpf3/1 probe) and the eye (optic vesicles).

Figure 3.13. WHISH expression analysis of Dpf3 with common, Dpf1 and DPF3/2 specific RNA *in situ* probes. Figure A E7.5 (ventral view), B-C E8.0 (frontal and left view), I E8.5 -section *in situ* hybridisation- (left view) and J E8.5 (ventral view) hybridisation results of common probe: cc-cardiac crescent, oft-outflow tract, ht-heart tube, ift-inflow tract, psm-presomitic mesoderm, v-ventricle, a-atrium, st-septum transversum, som-somite. Figure D E7.5 (ventral view), E-F and H E8.0 (frontal, left and ventral view) and K E8.5 (ventral view) of Dpf31 specific *in situ* hybridisation results. al-allantois, cc-cardiac crescent, nf neural fold, ht-heart tube, psm-presomitic mesoderm, cam-cardiac mesoderm bands (left and right), oft-outflow tract, v-ventricle, a-atrium, ift-inflow tract, al-allantois. Figure G E7.5 and L E8.5 (ventral view) were hybridised with Dpf3/2 specific *in situ* hybridisation probe.

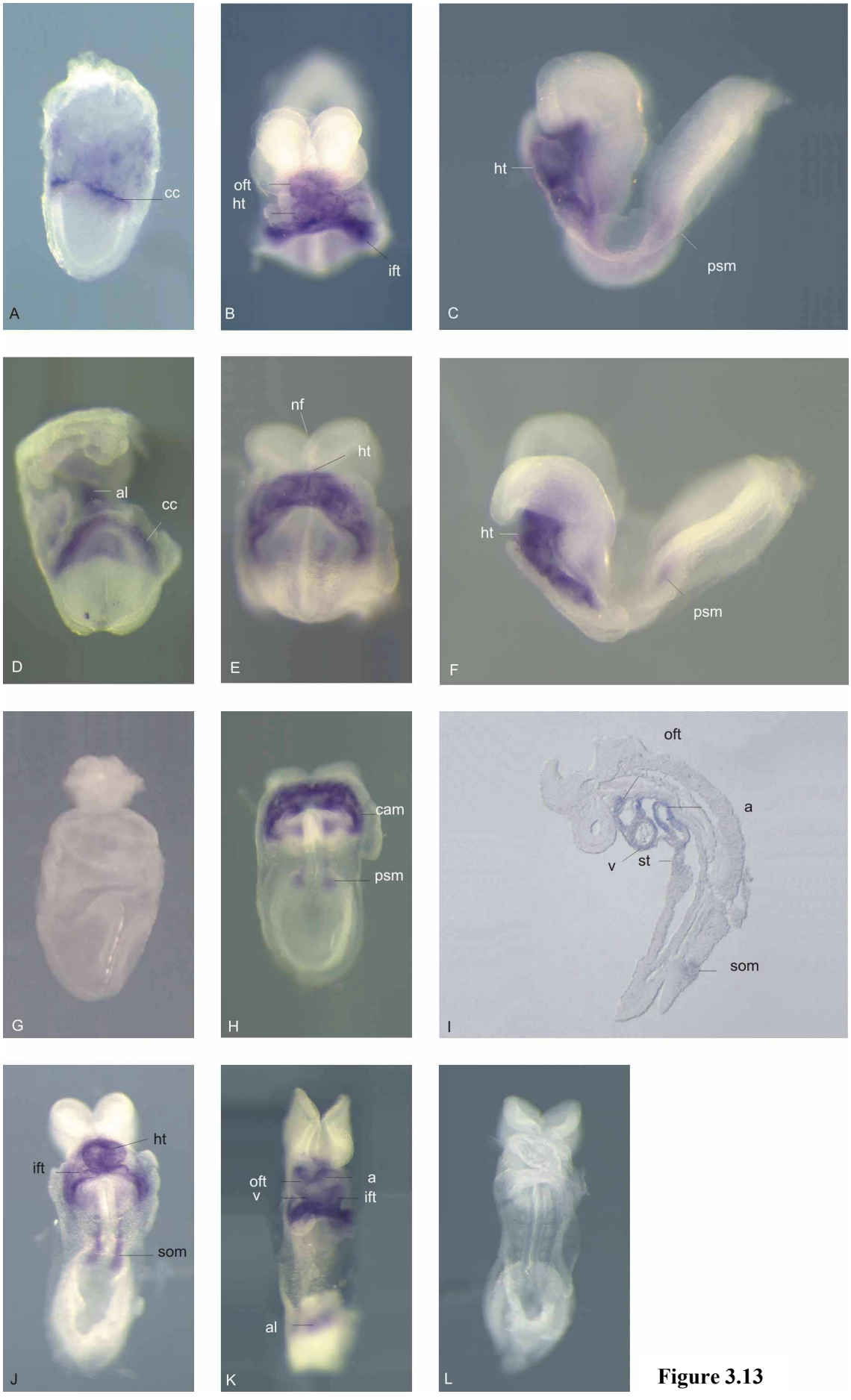
A
cc
B
oft
ht
ift
C
ht
psm
D
al
cc
E
nf
ht
F
ht
psm
G
H
cam
psm
I
oft
a
v
st
som
J
ht
ift
som
K
oft
v
a
ift
al
L

Figure 3.13

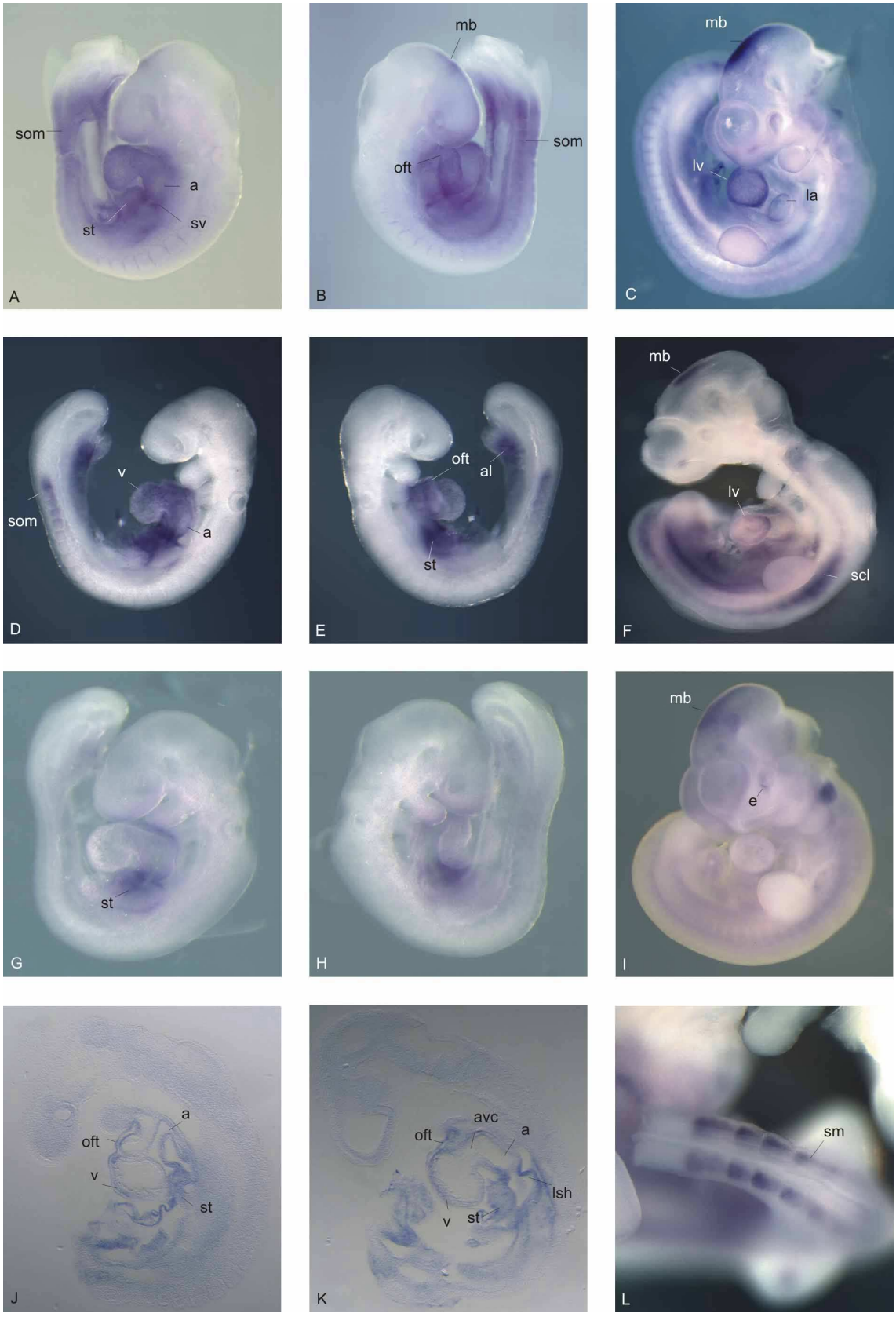
som
a
st
sv
A
mb
som
oft
B
mb
lv
la
C
v
som
a
D
oft
al
st
E
mb
lv
scl
F
st
G
H
mb
e
I
a
oft
v
st
J
avc
oft
a
lsh
v
st
K
sm
L

Figure 3.14

Figure 3.14. A-B E9.5 (left and right view), C E10.5 (left view), J-K E9.5 –sectioned WISH embryos right side of midline and left side of midline- were hybridised with Dpf3 common probe. som-somite, st-septum transversum, sv-sinus venosus, a-atrium, la-left atrium, v-ventricle, oft-outflow tract, mb-mid brain, lv-left ventricle, avc-atrioventricular channel, lsh-left sinus horn. D-E E9.5 (left and right view), F and L E10.5 (view from left and the tail) were hybridised with Dpf3/1 specific probe. som-somite, lv-left ventricle, a-atrium, oft-outflow tract, st-septum transversum, al-allantois, scl-sclerotome, mb-midbrain, som-somite. G and H E.9.5 (left and right view), I E11.5 (left view) were hybridised with RNA *in situ* probe Dpf3/2. st-septum transversum, e-eye, mb-midbrain.

For a more detailed observation of the Dpf3 gene expression pattern, embryonic hearts were extracted from the body and hybridised with the same *in situ* probe set. For the common probe (Figure 3.15A, B - E10.5) expression was observed in atrial and ventricular compartments of the heart, outflow tract and liver. Posterior-lateral walls of the ventricles as well as the outflow tract showed gradual staining. At E11.5, with the Dpf3/1 (Figure 3.15D) and the common probe (Figure 3.15C) expression was detected at the interventricular channel and the posterior-lateral sides of the ventricles and a very weakly staining observed at the outflow tract. The Dpf3/2 probe did not show any expression in cardiac compartments (Figure 3.15F).

Figure 3.15. A and B E10.5 (left and right view), C E12.0 (anterior view) extracted hearts were hybridised with Dpf3 common probe. lv-left ventricle, oft-outflow tract, rv-right ventricle, lv-left ventricle, ra-right atrium. D E12.0 extracted heart were hybridised with Dpf3/1 specific probe (anterior view). E and F E12.5 (frontal, left and right view) extracted hearts were hybridised with Dpf3/2 RNA *in situ* probes.
G and H E10.5 embryo (left and right view) was hybridised with Dpf1. tcl-telencephalon, e-eye, fba-first branchial arch, sba-second branchial arch, nt-neural tube, mb-mid brain, som-somite, npc-nephric chord, fl-forelimb. I, J E10.5 (left and right view) was hybridised with Dpf2 *in situ* hybridisation probe. tcl-telencephalon, fba-first branchial arch, sba-second branchial arch, som-somite, npc-nephric chord, fl-forelimb.

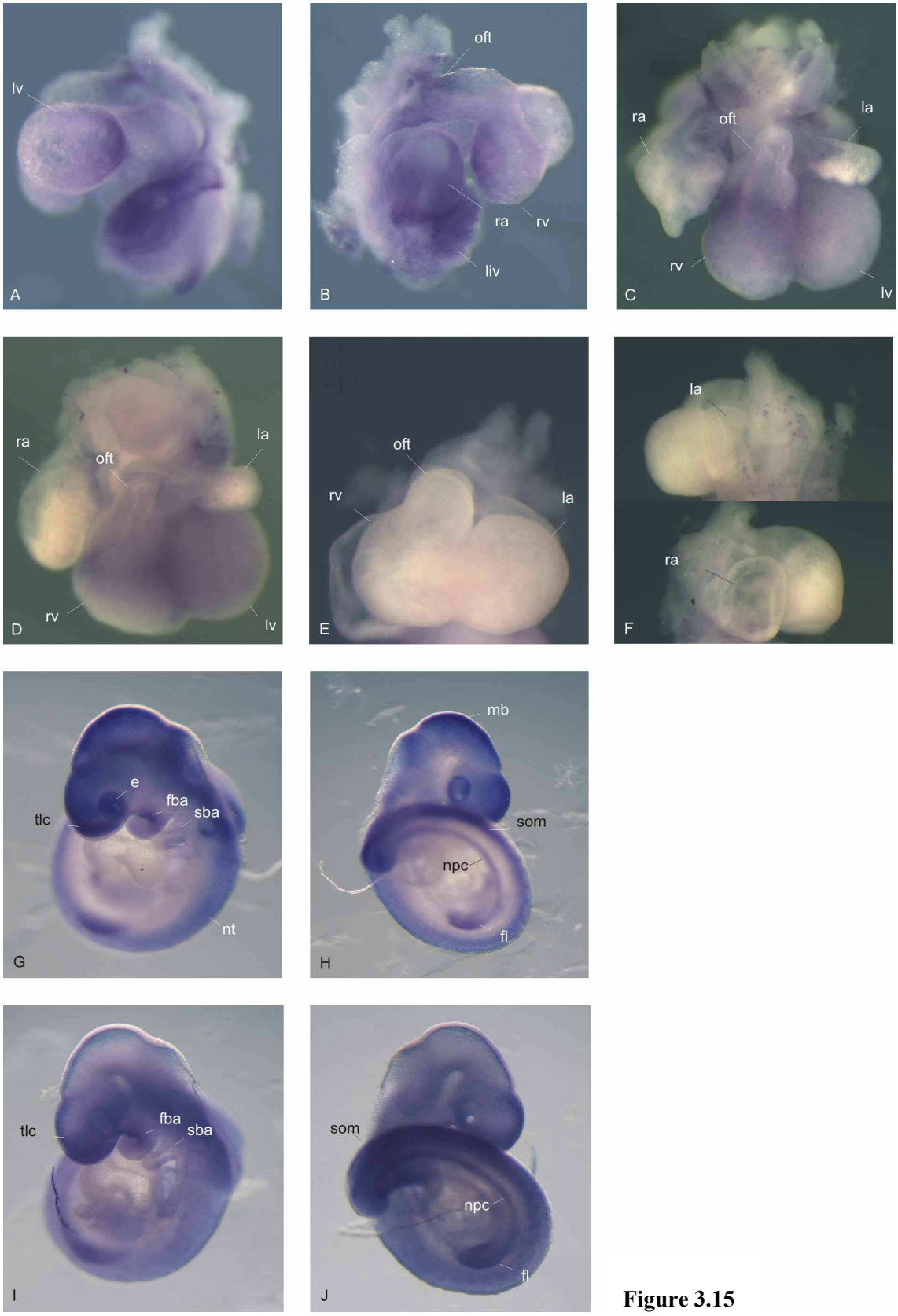
lv
A
oft
ra
rv
liv
B
ra
oft
la
rv
lv
C
ra
oft
la
rv
lv
D
oft
rv
la
E
la
ra
F
e
fba
sba
tlc
nt
G
mb
som
npc
fl
H
fba
sba
tlc
I
som
npc
fl
J

Figure 3.15

3.2.7 Chicken Dpf3 Splice Variants

The chicken Dpf3 homolog is characterised by four different splice variants. AF3620755 represents splice variant 1 and AF3620753 represents splice variant 2 compared to mouse and human, respectively. The additional two splice variants are derivations of Dpf3/1 and Dpf3/2 in mouse and human containing sequence insertions of 108bp and 39bp in length. The 108bp insertion-1 is localised between mouse/human exon 3 and exon 4 and the 39bp insertion-2 in-between mouse/human exon 5 and exon 6. AF3620756 is corresponding to the Dpf3/1 splice variant, additionally carrying insertion-2 and will therefore be called splice variant Dpf3/1a. AF3620754 corresponds to the Dpf3/2 splice variant carrying insertion-1 and insertion-2 and will be referred to as splice variant Dpf3/2a. As shown in figure 3.16, 226bp common region, 235bp Dpf3/1 and Dpf3/1a, 245bp Dpf3/2 and Dpf3/2a specific fragments were amplified from chicken embryonic heart cDNA. Also, a Dpf3/2a specific 279bp PCR product containing insert-1 and a Dpf3/2a and Dpf3/1a specific product containing insert-2 were detected in embryonic heart cDNA by RT-PCR (Figure 3.16).

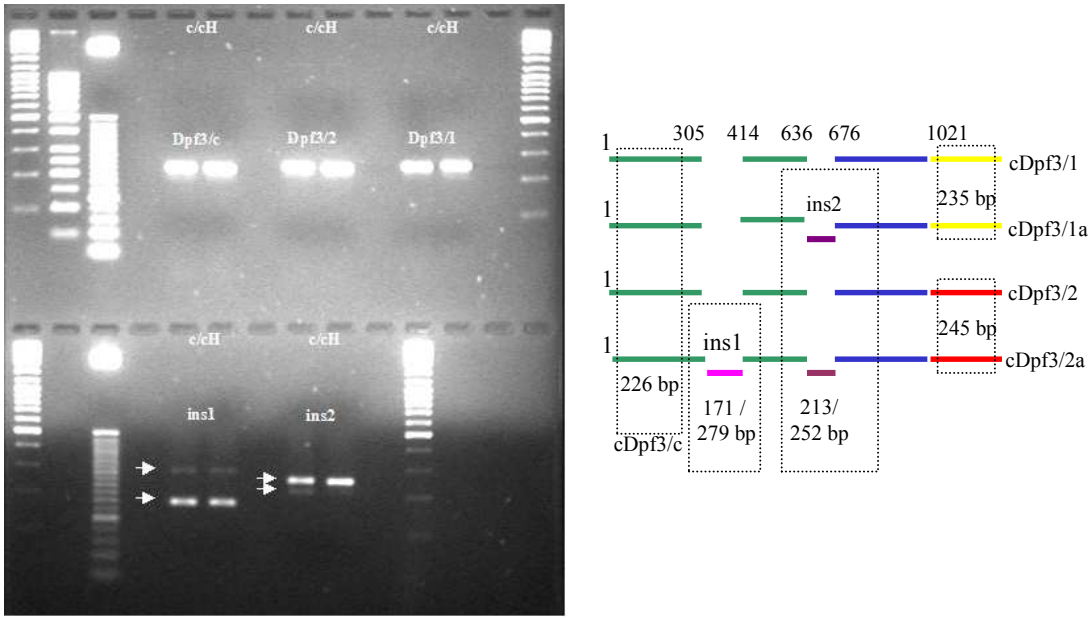

Figure 3.16. RT-PCR analysis of chick Dpf3 transcripts at E5.5 embryonic hearts. c-chick body, cH-chick heart. cDpf3/c-common region, ins1-insertion1, ins2-insertion2, green bars correspond to exons 1-5 of mouse and human, blue bars are indicating exons 6-8 of their homologue in mouse and human, yellow bars are showing the splice variant 1 (cDpf3/1) and red bars determine the splice variant 2 (cDpf3/2). Given numbers in boxes indicate the length of the amplified regions.

3.2.8 Expression Pattern of Dpf3 during Development in Chicken

A RNA *in situ* hybridisation probe was synthesised for the common region of the chicken Dpf3. Hybridisations were carried out for key developmental stages concerning early heart development of the chicken.

At HH4 (Hamburger and Hamilton staging) expression was observed in the prechordal plate mesoderm and foregut pocket (Figure 3.17A,B) located originally anterior of the Hensen node before the node started to migrate caudally. At stage HH7 (Figure 3.17C,D), staining was seen in prechordal plate mesoderm, foregut pocket and in addition in anterior intestinal portal. HH8 embryos showed Dpf3 expression at the prechordal plate mesoderm and foregut pocket (Figure 3.17E-F). At stage HH10 (Figure 3.18A-C) staining was observed in prechordal plate mesoderm, foregut pocket, and sinus venosus including atrium and vitellin veins. At stage HH12 (Figure 3.18D-F), expression was observed to be restricted to sinus venosus, vitellin veins including anterior intestinal portal, atrioventricular groove and weakly detected in the ventricle. The neural tube was also stained. Figures 3.18G and H show the left view of an HH16 stage embryo. Atrium, sinus venosus, anterior intestinal portal showed strong Dpf3 expression, outflow tract and ventricular region were stained weakly compared to the other parts of the cardiac region. In addition, optic vesicle, intermediate mesoderm, neural tube and gut endoderm were stained.

Chicken embryos at stage HH25 and HH30 were processed with radioactive and non-radioactive section *in situ* hybridisations.

At stage HH25, the sagital wax section passes from the left side of the midline showing expression of the Dpf3 common probe in the atrium, ventricle and sinus venosus as well as in the eyes (Figure 3.19A,C). At Figure 3.19B and D, sagital section of a stage HH30 embryo showed expression in the atrium, ventricle, trabecular region of ventricle, sinus venosus, mesencephalon, diencephalon, telencephalon, liver, stomach and mesonephros region.

In sagital cryo-sections of stage HH25 embryonic hearts were hybridised with non-radioactive RNA *in situ* hybridisations probe (DIG-labelled). Expression of Dpf3 was observed in the myocardium of the dorsal region of the atrium and anterior part of the ventricle, very weakly in the atrioventricular channel and in the initial connection of the outflow tract to the ventricle (Figure 3.19E,F).

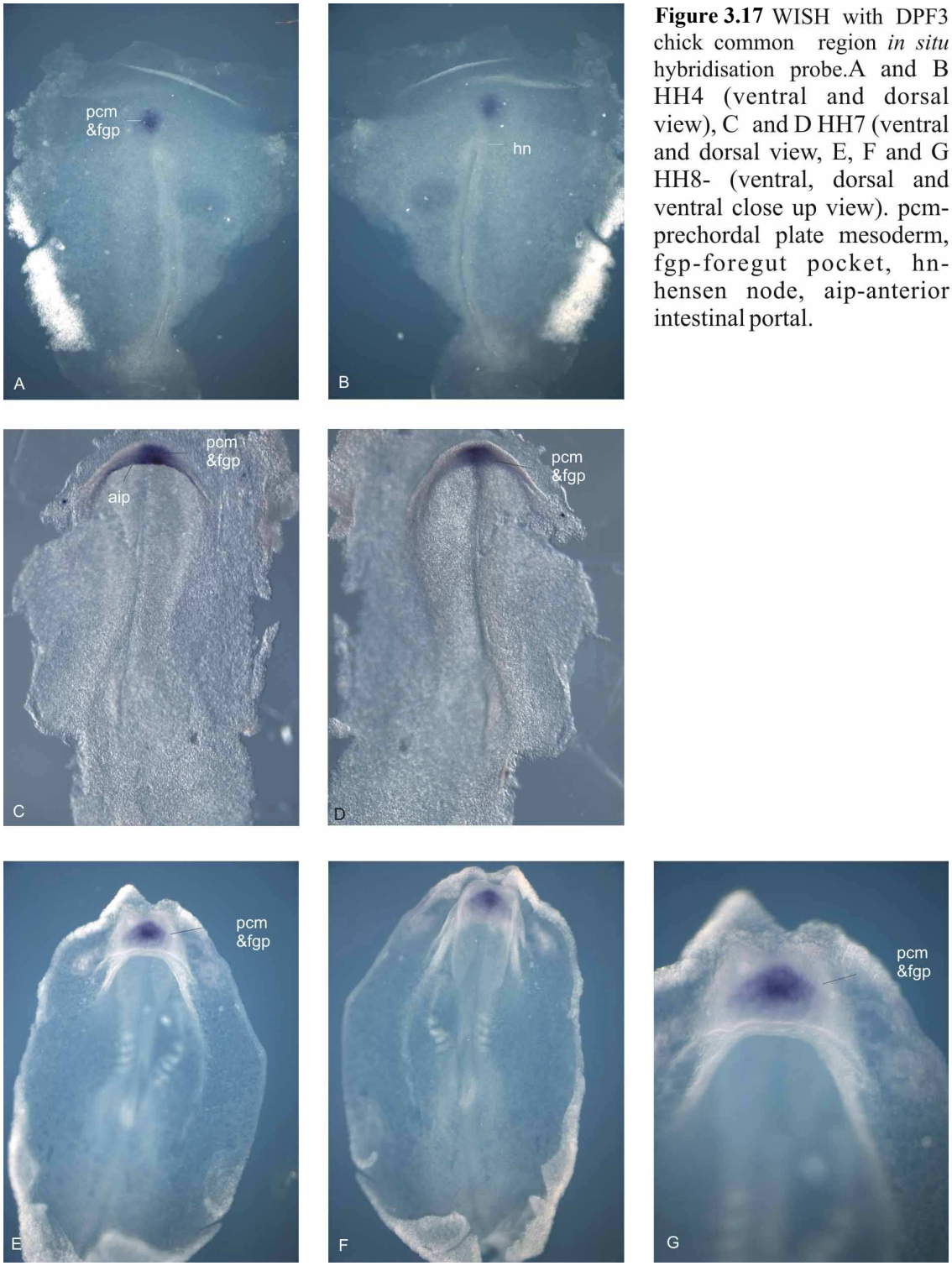

Figure 3.17 WISH with DPF3 chick common region *in situ* hybridisation probe.A and B HH4 (ventral and dorsal view), C and D HH7 (ventral and dorsal view, E, F and G HH8- (ventral, dorsal and ventral close up view). pcm-prechordal plate mesoderm, fgp-foregut pocket, hn-hensen node, aip-anterior intestinal portal.

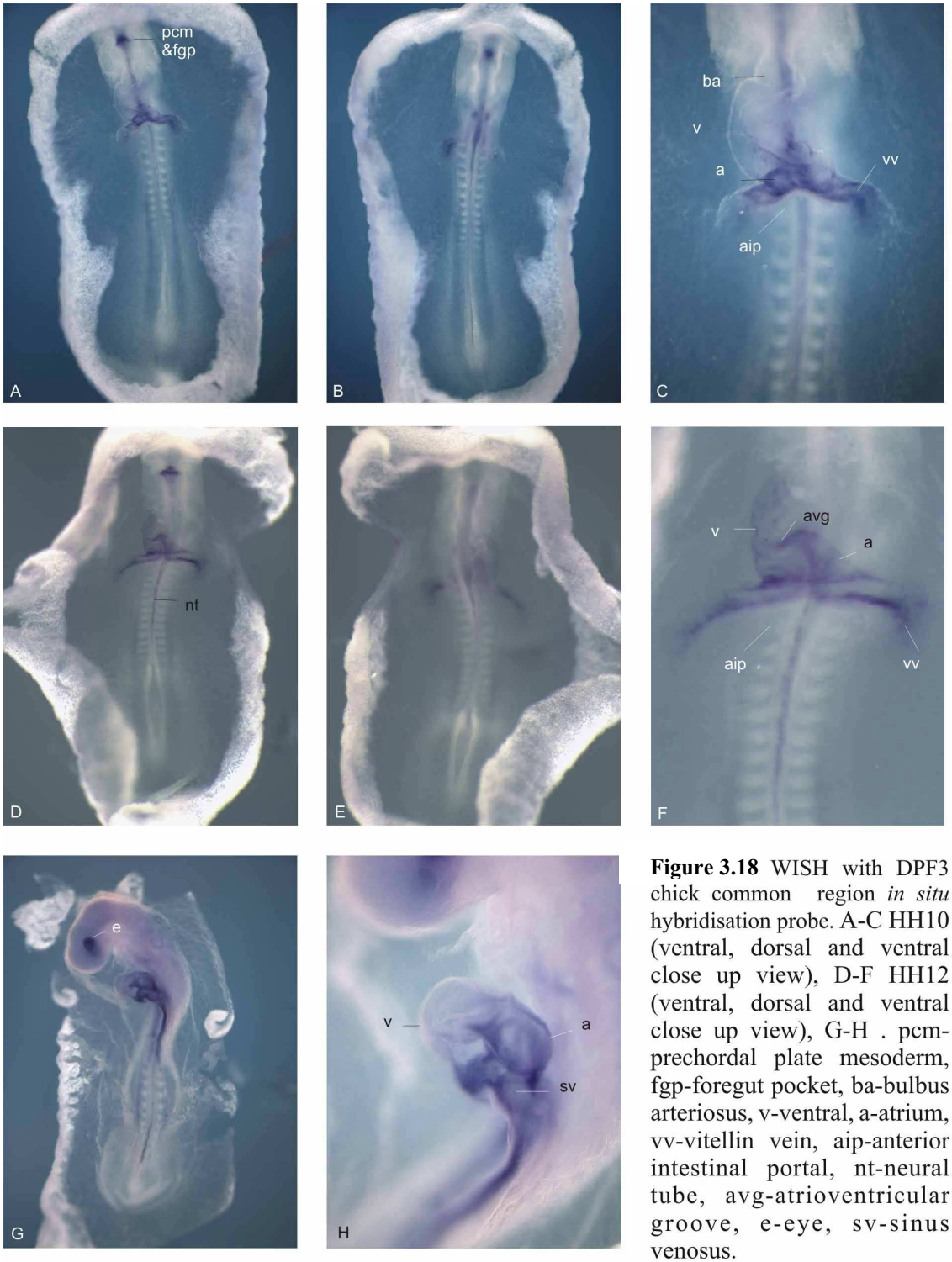

Figure 3.18 WISH with DPF3 chick common region *in situ* hybridisation probe. A-C HH10 (ventral, dorsal and ventral close up view), D-F HH12 (ventral, dorsal and ventral close up view), G-H . pcm-prechordal plate mesoderm, fgp-foregut pocket, ba-bulbus arteriosus, v-ventral, a-atrium, vv-vitellin vein, aip-anterior intestinal portal, nt-neural tube, avg-atrioventricular groove, e-eye, sv-sinus venosus.

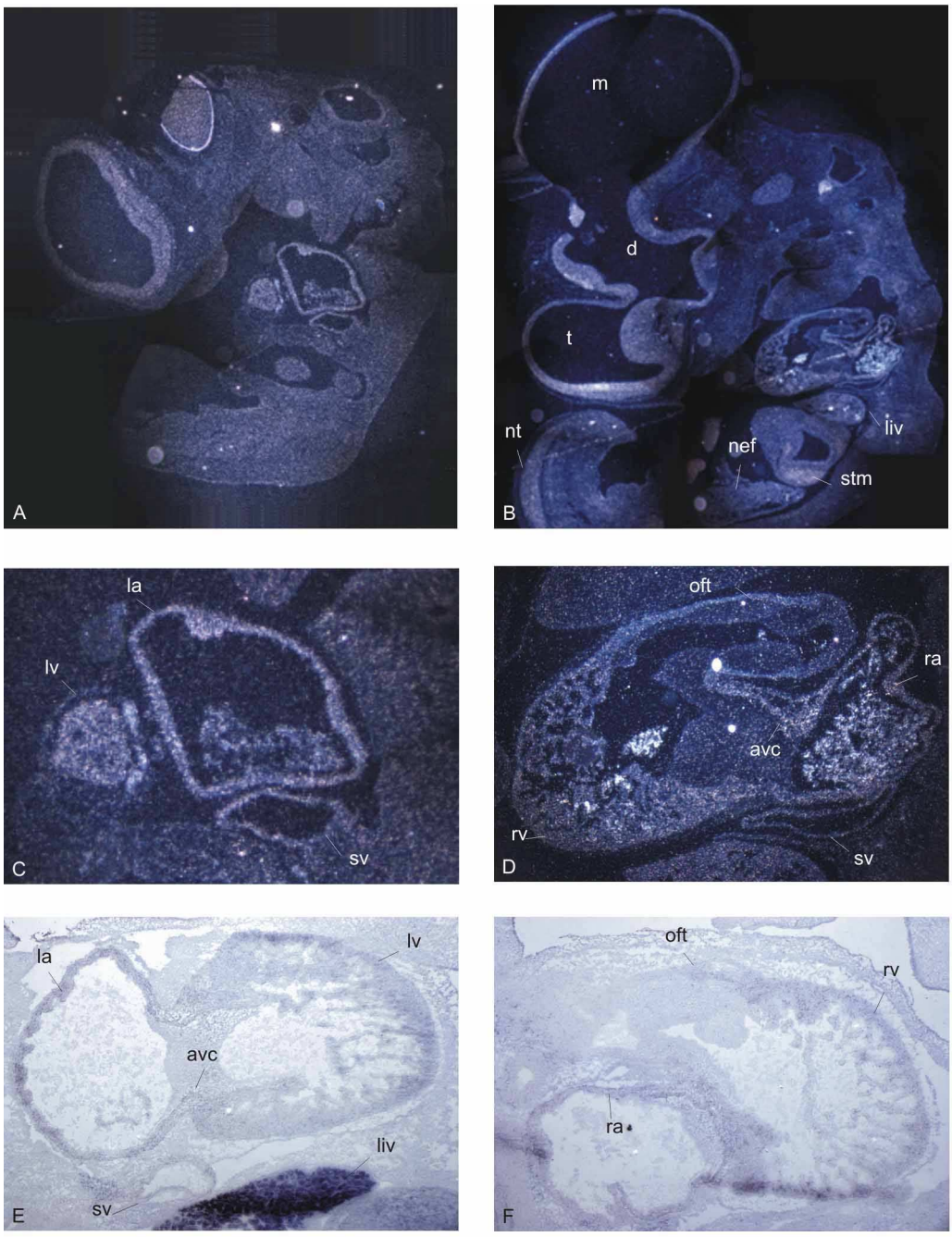

Figure 3.19 DPF3 chick common region specific radioactive RNA *in situ* hybridisation probe. was hybridised with A and C HH25 (section passed from right side of midline, C is close up to the heart), B-D HH30 (section passed from left side of midline, D is close up to the heart.
DPF3 chick common region specific non radioactive RNA *in situ* hybridisation probe was hybridised with HH25 cryo sections. E, section from right side of midline and F, section from the left side of the embryo.
la-left atrium, lv-left ventricle, avc-atrioventricular channel, sv-sinus venosus, liv-liver, oft-outflow tract, ra-right atrium, rv-right ventricle, nef- mesonephros, stm-stomach, m-mesencephalon, d-diencephalon, t-telencephalon, nt-neural tube.

3.2.9 Retinoic Acid Treatment in Chicken Embryo Culture

Following the all-*trans*-retinoic acid treatment (RA), embryos were processed and hybridised with the Dpf3 common probe by whole mount RNA *in situ* hybridisation. Figure 3.20A-C shows the expression of DPF3 in a non-treated control. Sinus venosus, vitellin veins, atrium, anterior intestinal portal parts of cardiac mesodermal bands were stained in addition to weakly ventricle restricted brain expression in mesencephalon and neural tube. In comparison to non RA treated embryos, treated ones (10^{-4}M RA treated) showed morphological changes, such as weakly altered cardiac looping, thickening of the cardiac venous pool and dysdevelopment of the anterior brain portion. Apart from the rearrangements in development of the body axis, Dpf3 expression was increased at the sinus venosus, anterior intestinal portal and the cardiac mesodermal bands. Expression in the vitellin veins remained the same. Furthermore, treatment of RA lead to altered neural tube expression of Dpf3 (Figure 3.20D-F).

Application of a double amount of RA [$2x10^{-4}$M] caused severe dysdevelopment of the embryo concerning anterior-posterior patterning and resulted in incomparable morphology in contrast to similar expression of control non-cultured and non-treated embryos (Figure 3.20G-H). Dpf3 expression was observed at the sinus venosus region and the posterior stripes followed by vitellin veins. Brain expression was altered due to the rearrangements of the embryonic body axis and anterior-posterior patterning.

Figure 3.20. WISH with Dpf3 chick common region *in situ* hybridisation probe. A-C HH~11 cultured but not RA treated (ventral, dorsal and ventral close up view), D-F HH~11 cultured and 10^{-4}M RA treated embryo (ventral, dorsal and ventral close up view), G-I cultured and $2x10^{-4}$M RA treated embryo (anterior-lateral, anterior-dorsal, ventral close up view). nt-neural tube, v-ventricle, a-atrium, sv-sinus venosus, aip-anterior intestinal portal, cmb-cardiac mesodermal bands, ht-heart tube.

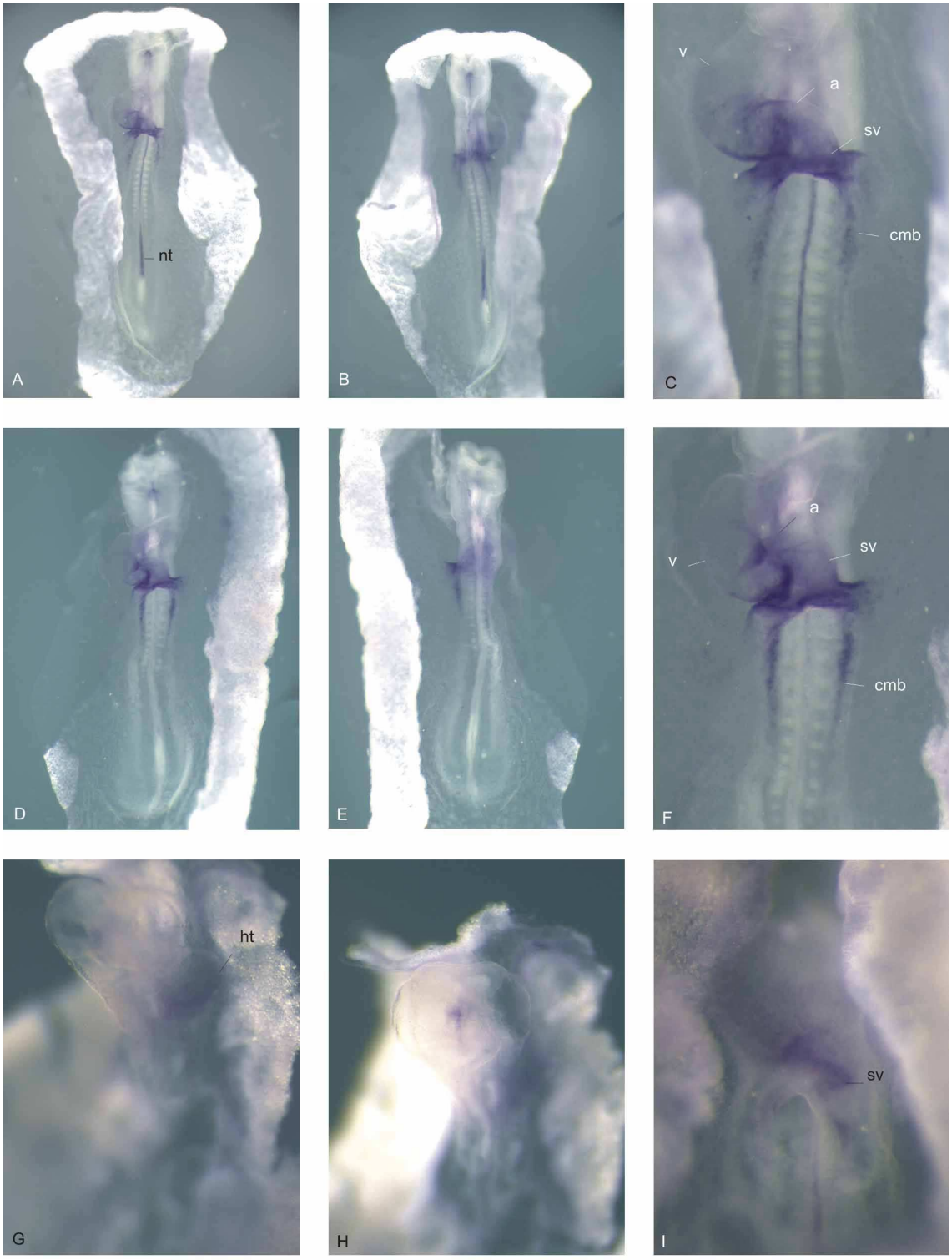

Figure 3.20

3.2.10 Zebrafish Dpf3 Splice Variants

Zebrafish Dpf3 is localised on chromosome 20 and spans 39.2 Mb. There are four transcripts of Dpf3 of which three are characterised by conserved sequences in comparison to human, mouse and chicken. Figure 24 shows the multiple alignment of different splice variants of zebrafish Dpf3. ENSDART00000034193 corresponds to splice variant 1 in human, mouse and chicken and contains sequence variations in-between base pair position 274 and 492. ENSDART00000034245 represents splice variant 2 in zebrafish with variations in-between 274-492bp. ENSDART00000034310 is another splice variant 2 derivative and contains sequence variations in between position 274:492bp and 802:827bp and ENSDART00000034334 is the last derivative of the splice variant 2 and it is lacking the proper double PHD domain due to the missing sequence at position 664bp and 802bp.

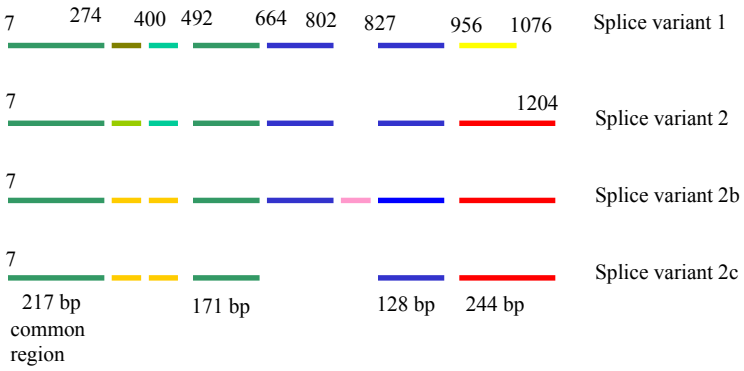

Figure 3.21. Multiple alignment of Dpf3 splice variants in Zebrafish. Each colour represents the conserved regions at nucleic acid level. Dark green represents the common region corresponding to exon 1 to 5 of human, mouse and chicken. The blue colour corresponds to exon 6 to 8 in the same respect. Red defines the splice variant 2 and light yellow represents the splice variant 1. Other colours represent variations in the organisation of Dpf3 transcripts in Zebrafish.

To characterise the expression pattern of the zebrafish Dpf3 gene, a series of whole mount *in situ* hybridisations were done and compared to the expression of the well-known early cardiac marker zebrafish Nkx-2.5. For Dpf3 stage 24hpf and 33hpf were chosen. Zebrafish Nkx-2.5, stained at stage 24hpf was used as a control.

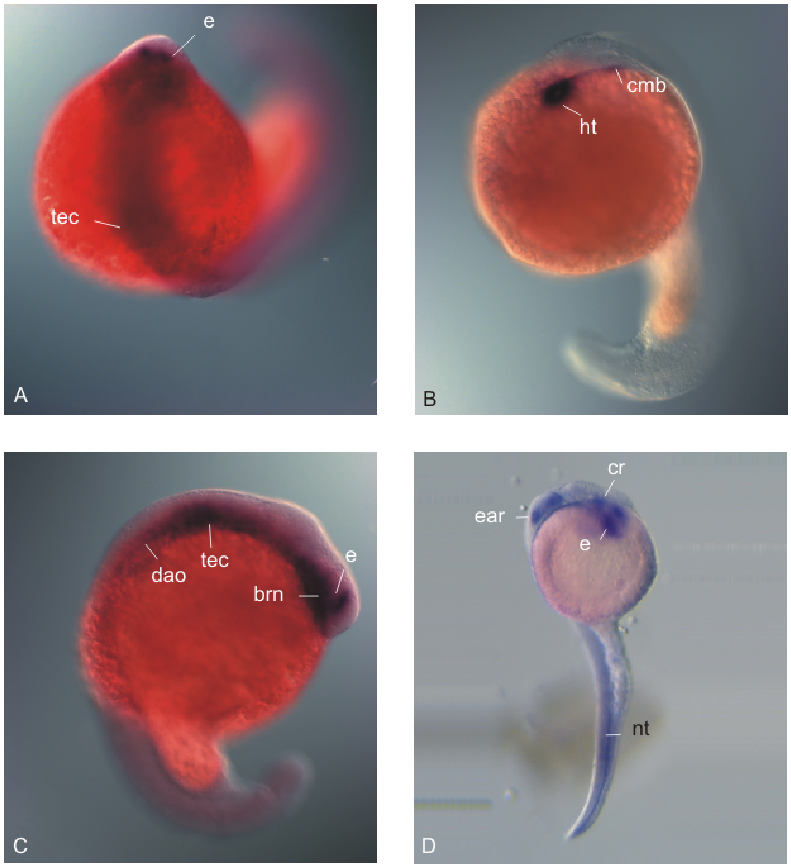

Figure 3.22. A,C 24 hpf (dorsal and left side view) hybridised with zDpf3 common region, D 33hpf (right view), B 24 hpf zebrafish Nkx-2.5. e-eye, tec-tectum, dao-dorsal aorta, brn-brain, ht-heart tube, cmb-cardiac mesodermal band, ear, cr-cardiac region, nt-neural tube.

At stage 24hpf, Dpf3 was mainly expressed in tectum (sensory plate), as well as in eyes and brain. A possible cardiac staining was not distinguishable from the predominance of the brain expression due to the regional neighbouring. At stage 33hpf, staining was observed in eyes, ears and the neural tube. Cardiac staining was considered to be ambiguous.

3.2.11 D4 Family Members in Human and Mouse

Human DPF1 (NEUD4) is located on chromosome 19q13.13-q13.2 and gives rise to two transcripts containing 11 exons. It is also known as the first member of D4 family containing a zinc finger like PHD domain (INTERPRO, IPR001225). The Mouse ortholog Dpf1 is located on chromosome 7 and consists of 5 exons. A 301bp RNA probe was synthesised from adult mouse heart cDNA corresponding to NM_004647 sequence (1189-1483bp) and hybridised to E10.0 mouse embryos. Mouse Dpf1 showed

expression in telencephalon, midbrain, eyes, first and second branchial arches, neural tube, forelimbs, nephric chord and somites. The heart and the cardiovascular region were free of staining (Figure 3.15G, H).

Human DPF2 is the second member of D4 family, which is localised on chromosome 11q13.1. It is also known as UBID4 or REQUIEM. As DPF1, DPF2 also has zinc finger like PHD domain (IPR001965) and a C2H2 type zinc finger domain (IPR007087) like DPF3. The mouse ortholog of Dpf2 [GI: 21536317] is localised on chromosome 19. A 302bp RNA probe was prepared from adult mouse heart cDNA for *in situ* hybridisation corresponding to the NM_006268 sequence (326-629) and hybridised to E10.0 mouse embryos. Dpf2 shows expression in telencephalon, first and second branchial arches, forelimbs, somites, surface ectoderm and nephric chord. However, Dpf2 expression was not observed in the cardiac region (Figure 3.15I, J).